Chapter 4
Bases for Krylov subspaces

4.1 Orthonormal basis

4.2 Hessenberg basis

4.3 Biorthogonal basis

4.4 The generalized Hessenberg process

4.5 Q-OR optimal basis

4.6 Newton and Chebyshev bases

4.7 Truncated bases

4.8 Parallel computing

4.9 Finite precision arithmetic and numerical experiments

4.9.1 Orthogonal basis

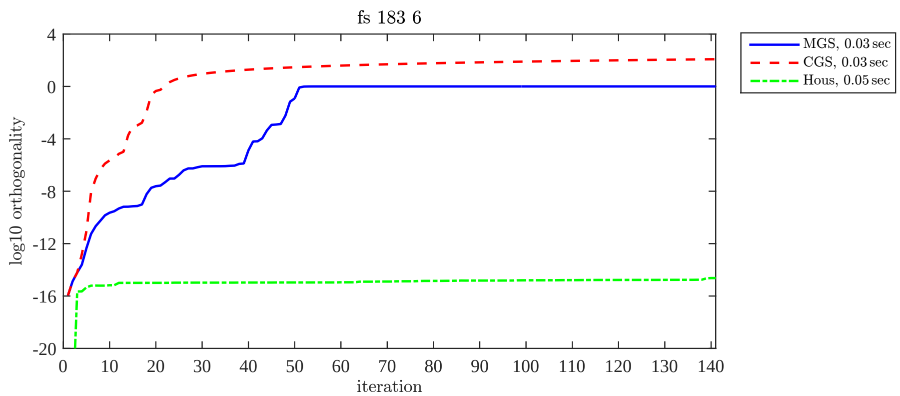

Fig. 4.1 fs 183 6, $\log_{10} \|I - V_{n,k}^T V_{n,k}\|$, Arnoldi MGS (plain), CGS (dashed), Householder (dot-dashed)

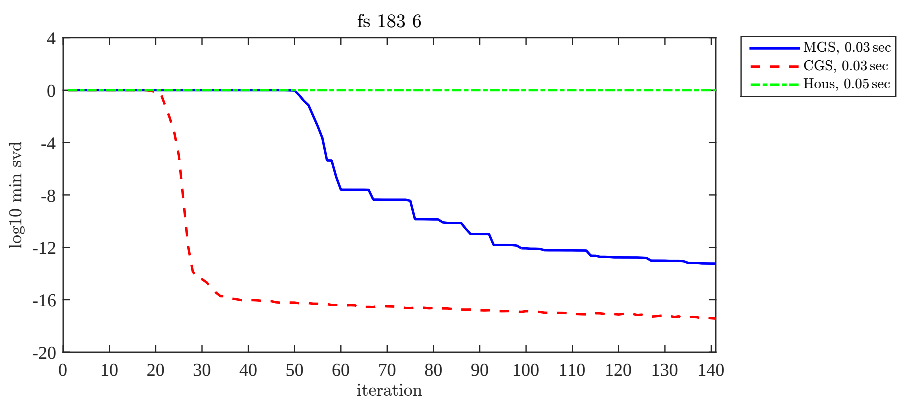

Fig. 4.2 fs 183 6, $\log_{10}$ of minimum singular value of $V_{n,k}$, Arnoldi MGS (plain), CGS (dashed), Householder (dot-dashed)

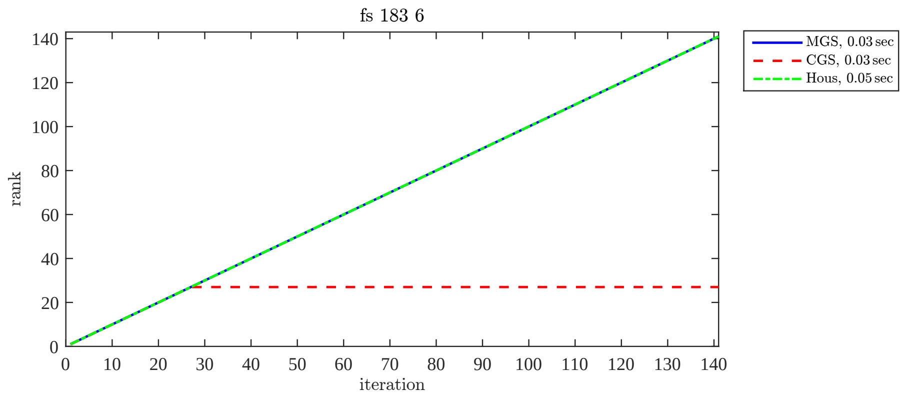

Fig. 4.3 fs 183 6, numerical rank of $V_{n,k}$, Arnoldi MGS (plain), CGS (dashed), Householder (dot-dashed)

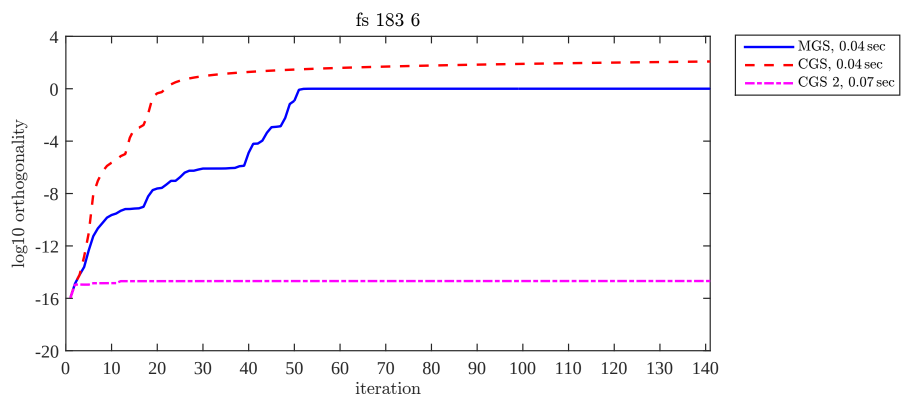

Fig. 4.4 fs 183 6, $\log_{10} \|I - V_{n,k}^T V_{n,k}\|$, Arnoldi MGS (plain), CGS (dashed), CGS with reorthogonalization (dot-dashed)

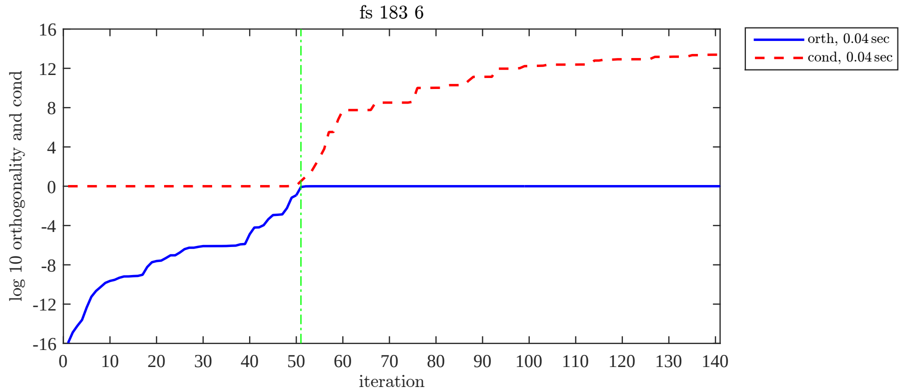

Fig. 4.5 fs 183 6, MGS, $\log_{10} \|I - V_{n,k}^T V_{n,k}\|$ (plain) and $\log_{10}$ of $\mathrm{cond}(V_{n,k})$ (dashed)

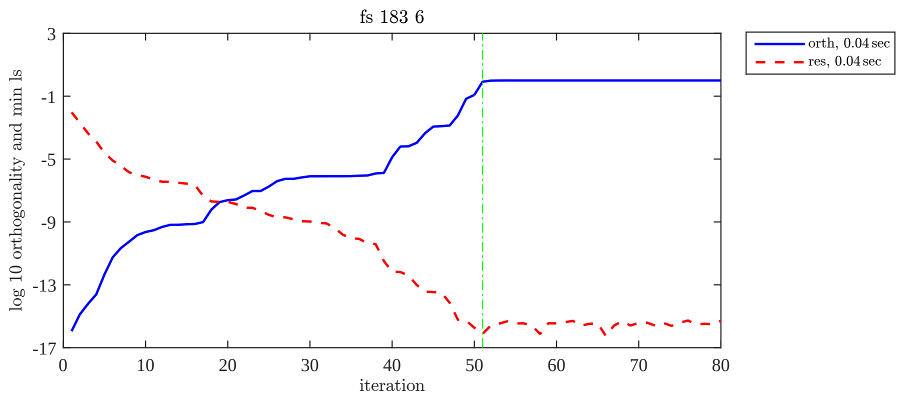

Fig. 4.6 fs 183 6, MGS, $\log_{10} \|I - V_{n,k}^T V_{n,k}\|$ (plain) and $\log_{10}$ of $\min_y \|v_1 - AV_{n,k}y\|$

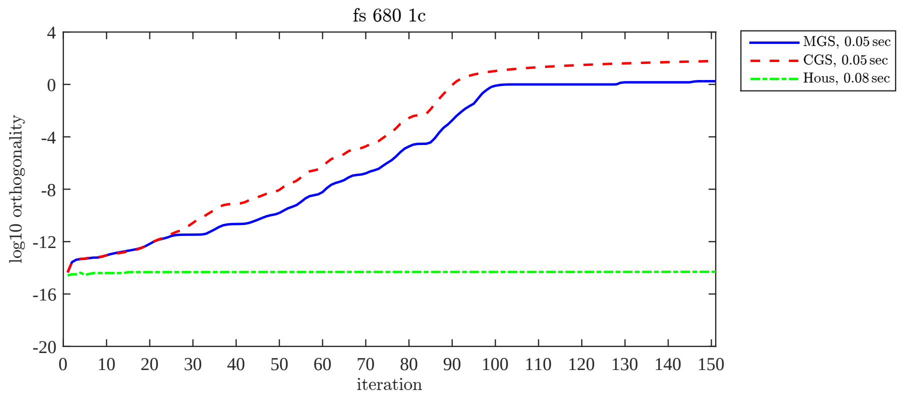

Fig. 4.7 fs 680 1c, $\log_{10} \|I - V_{n,k}^T V_{n,k}\|$, Arnoldi MGS (plain), CGS (dashed), Householder (dot-dashed)

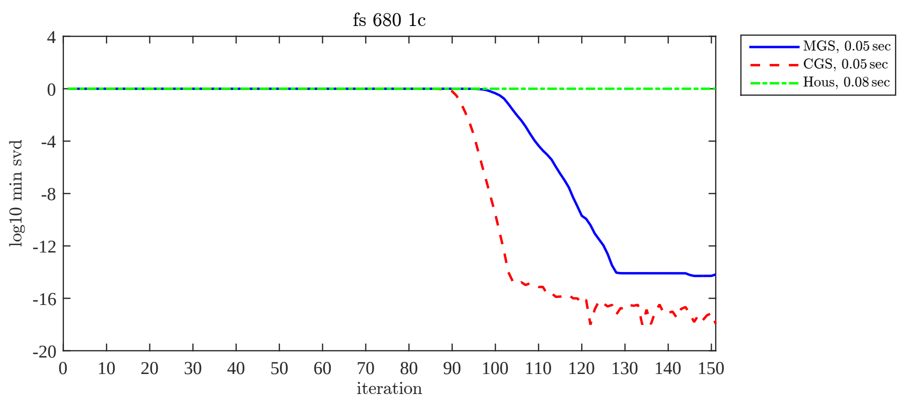

Fig. 4.8 fs 680 1c, $\log_{10}$ of minimum singular value of $V_{n,k}$, Arnoldi MGS (plain), CGS (dashed), Householder (dot-dashed)

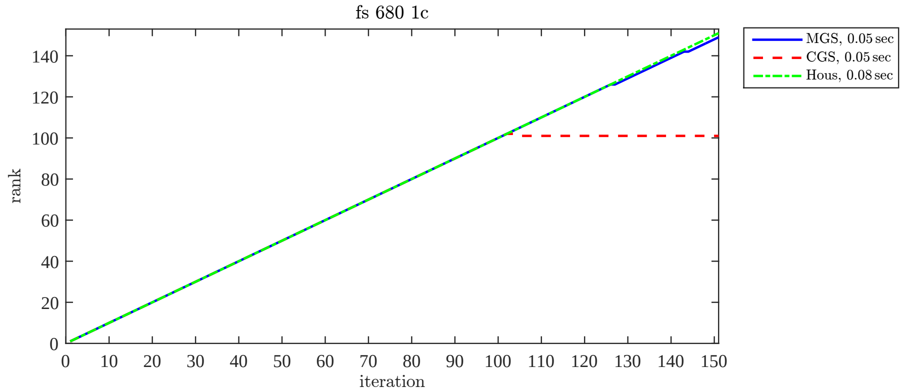

Fig. 4.9 fs 680 1c, numerical rank of $V_{n,k}$, Arnoldi MGS (plain), CGS (dashed), Householder (dot-dashed)

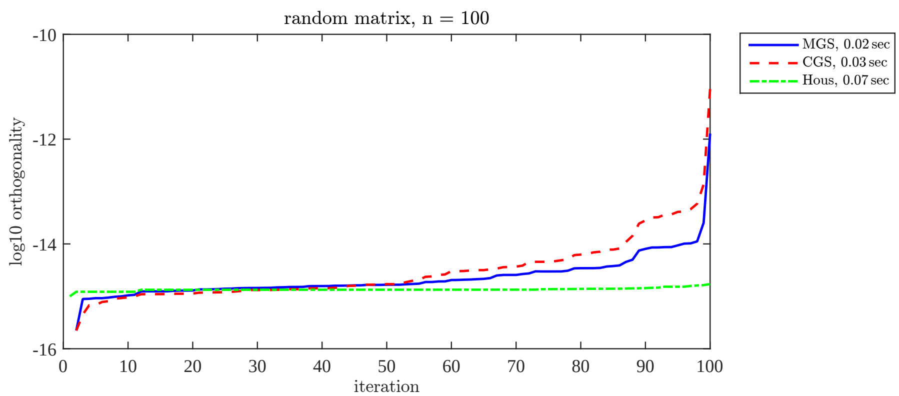

Fig. 4.10 random matrix $n = 100$, $\log_{10} \|I - V_{n,k}^T V_{n,k}\|$, Arnoldi MGS (plain), CGS (dashed), Householder (dot-dashed)

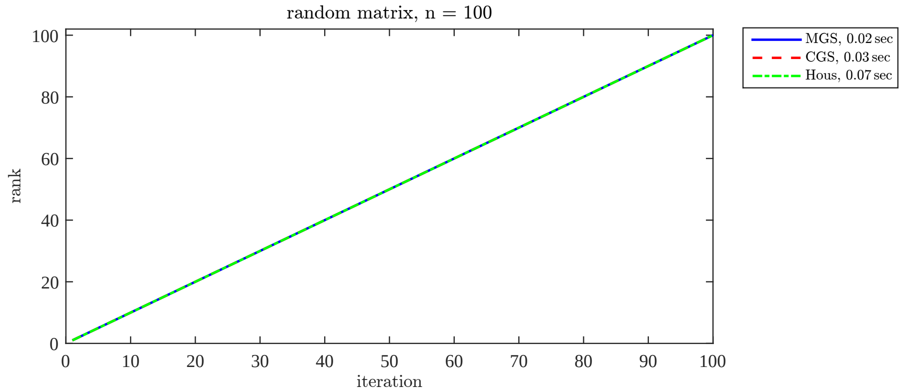

Fig. 4.11 random matrix $n = 100$, numerical rank of $V_{n,k}$, Arnoldi MGS (plain), CGS (dashed), Householder (dot-dashed)

4.9.2 Hessenberg basis

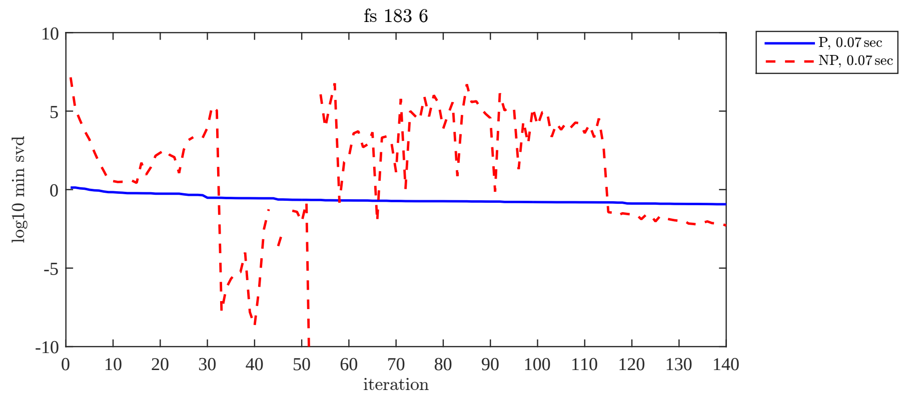

Fig. 4.12 fs 183 6, $\log_{10}$ of minimum singular value of $V_{n,k}$, Hessenberg with pivoting (plain), without pivoting (dashed)

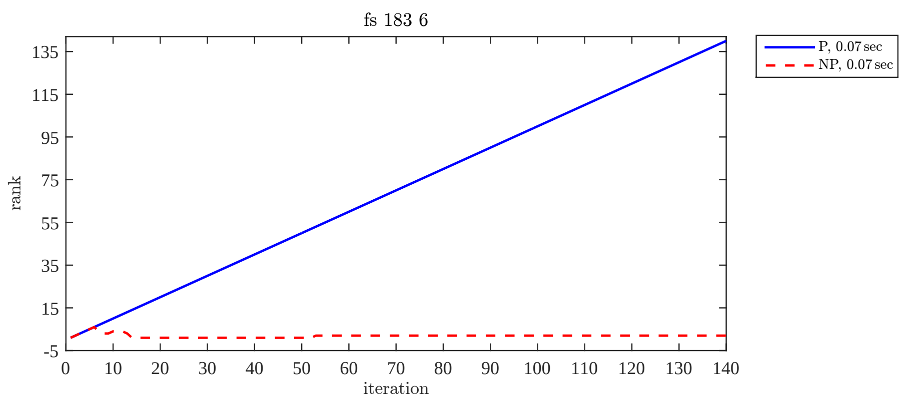

Fig. 4.13 fs 183 6, numerical rank of $V_{n,k}$, Hessenberg with pivoting (plain), without pivoting (dashed)

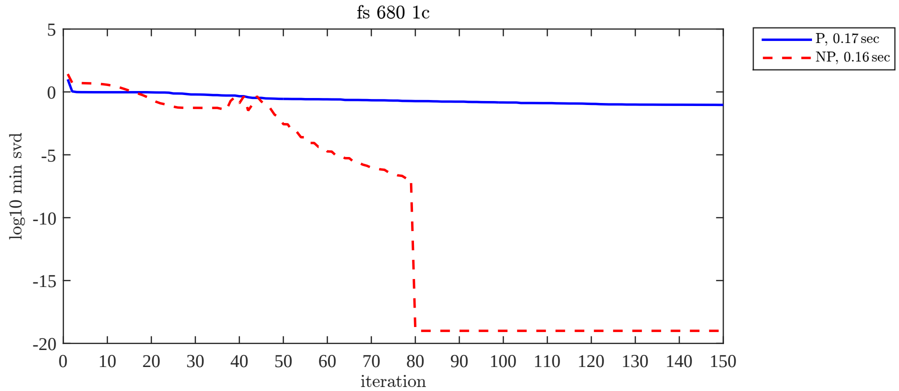

Fig. 4.14 fs 680 1c, $\log_{10}$ of minimum singular value of $V_{n,k}$, Hessenberg with pivoting (plain), without pivoting (dashed)

4.9.3 Biorthogonal basis

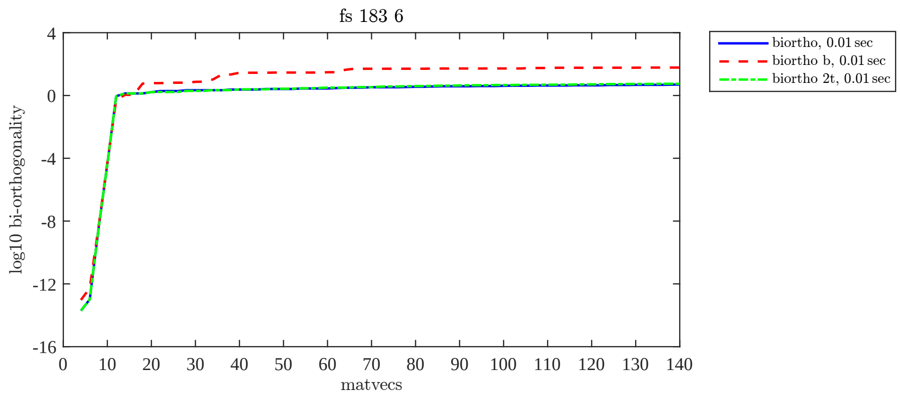

Fig. 4.15 fs 183 6, $\log_{10}$ of the level of biorthogonality, biortho (plain), biortho bis (dashed), biortho 2t (dot-dashed)

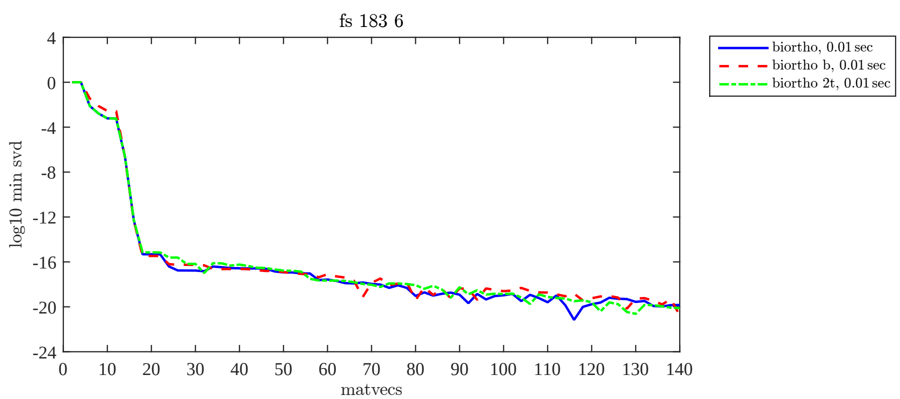

Fig. 4.16 fs 183 6, $\log_{10}$ of minimum singular value of $V_{n,k}$, biortho (plain), biortho bis (dashed), biortho 2t (dot-dashed)

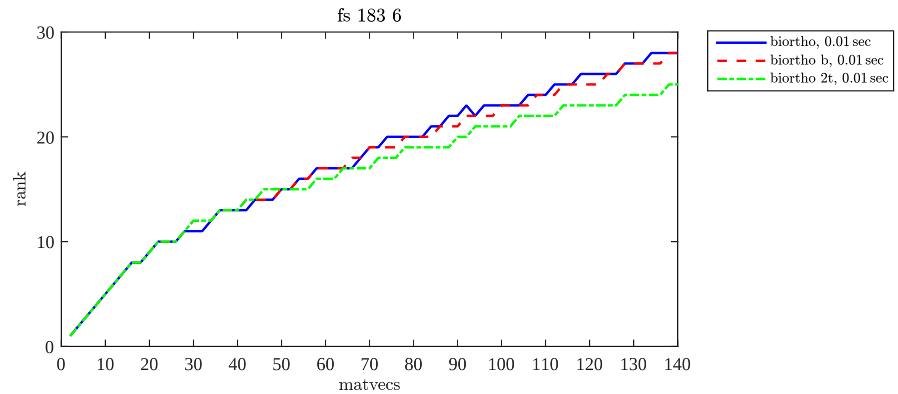

Fig. 4.17 fs 183 6, numerical rank of $V_{n,k}$, biortho (plain), biortho bis (dashed), biortho 2t (dot-dashed)

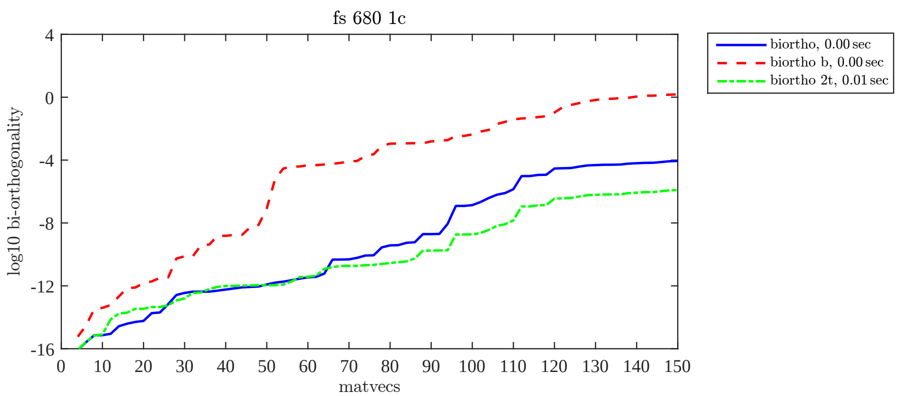

Fig. 4.18 fs 680 1c, $\log_{10}$ of the level of biorthogonality, biortho (plain), biortho bis (dashed), biortho 2t (dot-dashed)

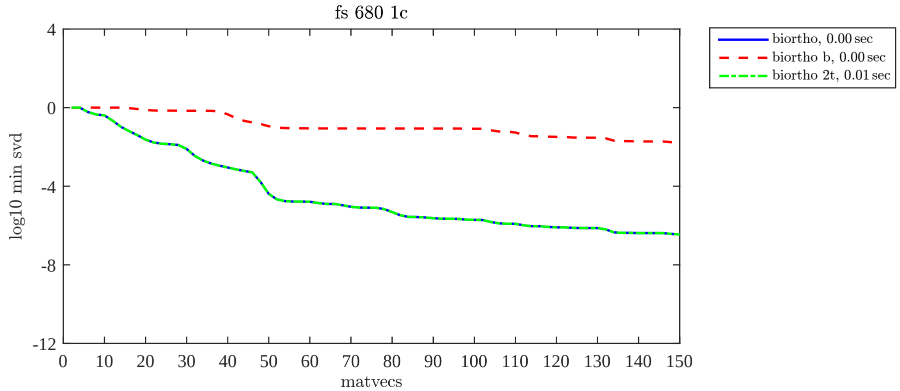

Fig. 4.19 fs 680 1c, $\log_{10}$ of minimum singular value of $V_{n,k}$, biortho (plain), biortho bis (dashed), biortho 2t (dot-dashed)

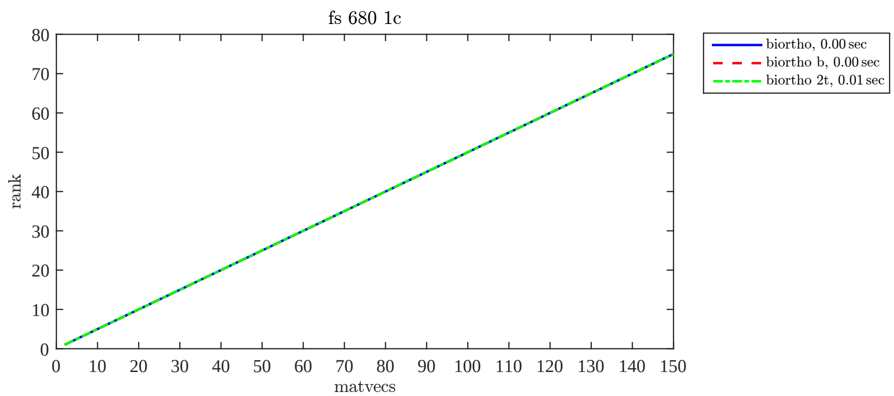

Fig. 4.20 fs 680 1c, numerical rank of $V_{n,k}$, biortho (plain), biortho bis (dashed), biortho 2t (dot-dashed)

4.9.4 Q-OR opt basis

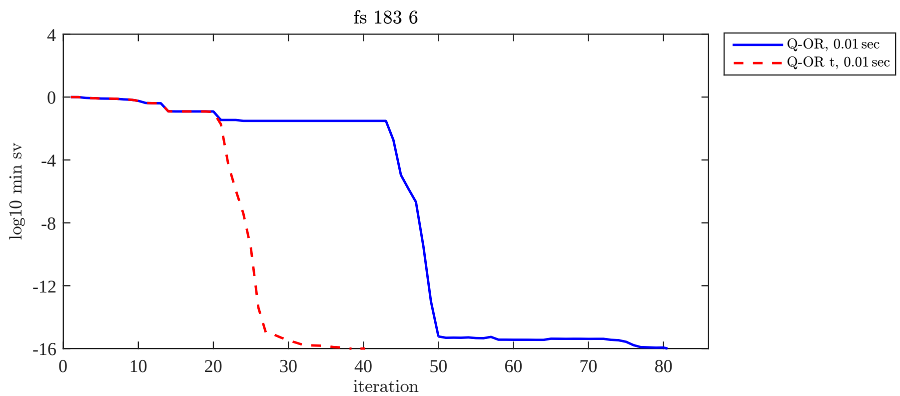

Fig. 4.21 fs 183 6, $\log_{10}$ of minimum singular value of $V_{n,k}$, Q-OR (plain), Q-OR t (dashed)

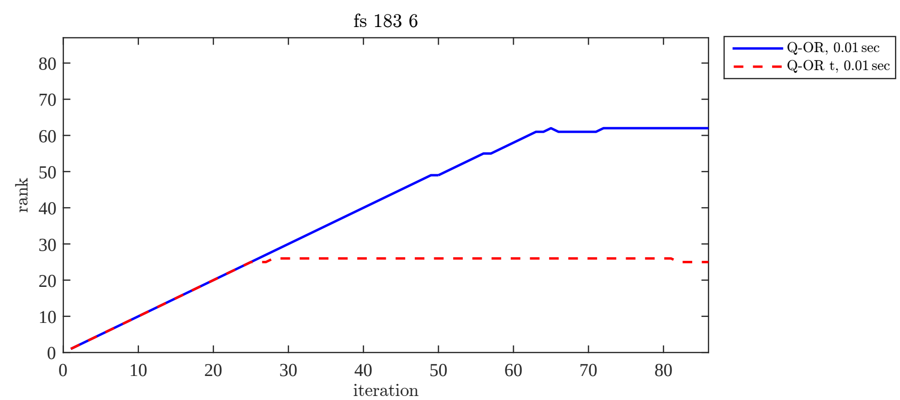

Fig. 4.22 fs 183 6, numerical rank of $V_{n,k}$, Q-OR (plain), Q-OR t (dashed)

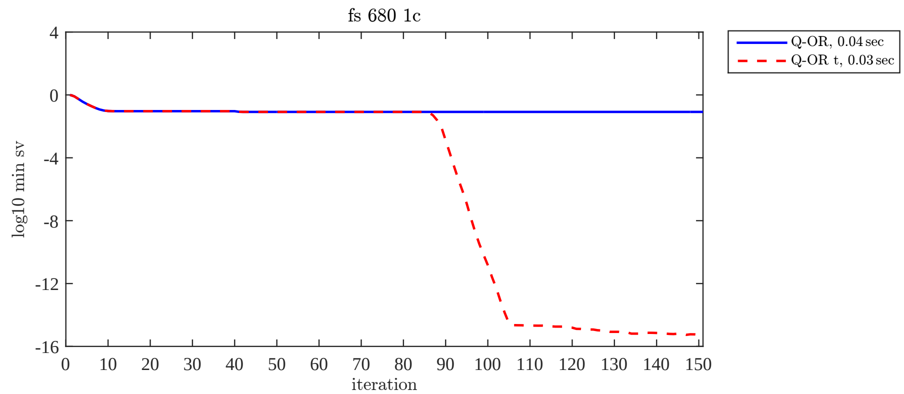

Fig. 4.23 fs 680 1c, $\log_{10}$ of minimum singular value of $V_{n,k}$, Q-OR (plain), Q-OR t (dashed)

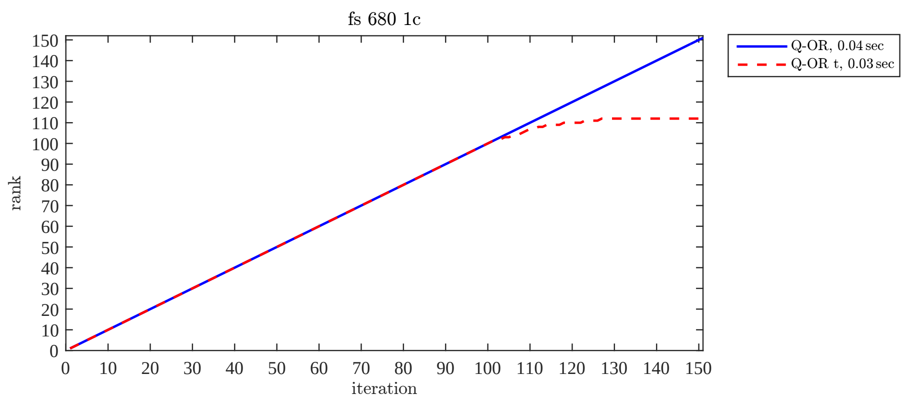

Fig. 4.24 fs 680 1c, numerical rank of $V_{n,k}$, Q-OR (plain), Q-OR t (dashed)

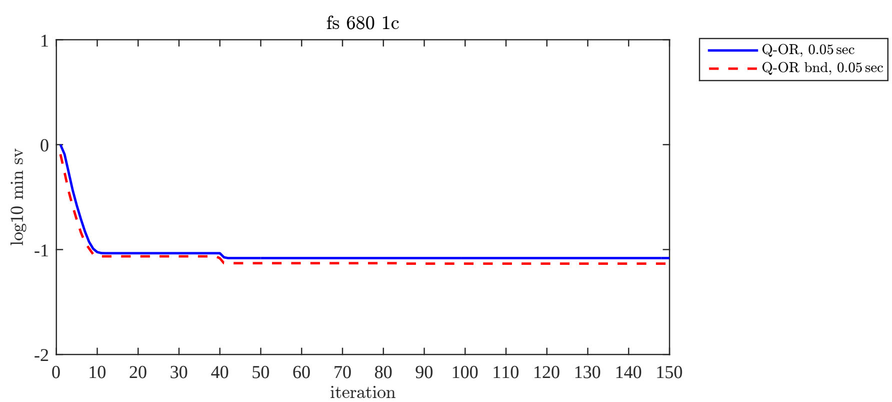

Fig. 4.25 fs 680 1c, $\log_{10}$ of minimum singular value of $V_{n,k}$ (plain) and lower bound (dashed)

4.9.5 Newton and Chebyshev bases

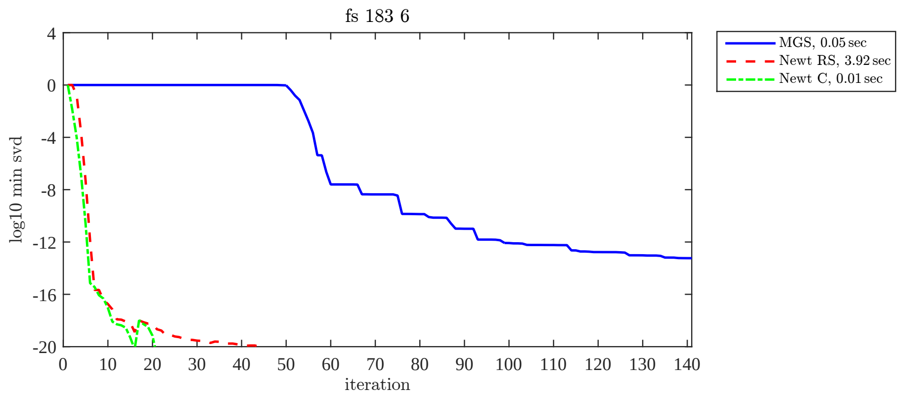

Fig. 4.26 fs 183 6, $\log_{10}$ of minimum singular value of $V_{n,k}$, Arnoldi (plain), Newton RS (dashed), Chebyshev (dot-dashed)

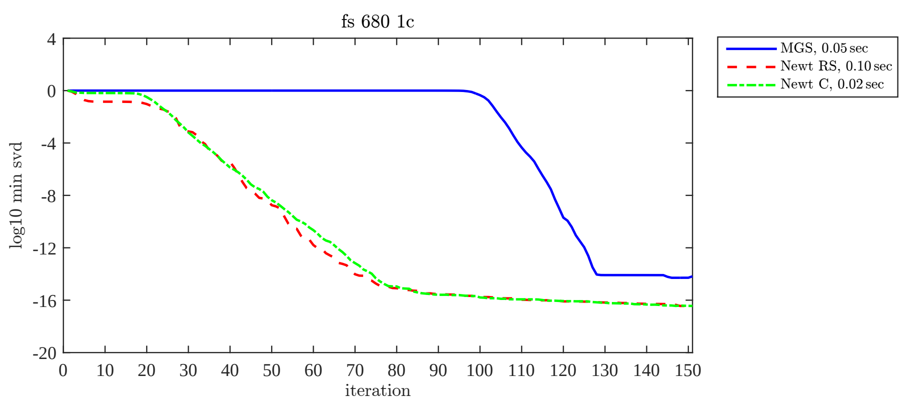

Fig. 4.27 fs 680 1c, $\log_{10}$ of minimum singular value of $V_{n,k}$, Arnoldi (plain), Newton RS (dashed), Chebyshev (dot-dashed)

4.9.6 Truncated Q-OR basis

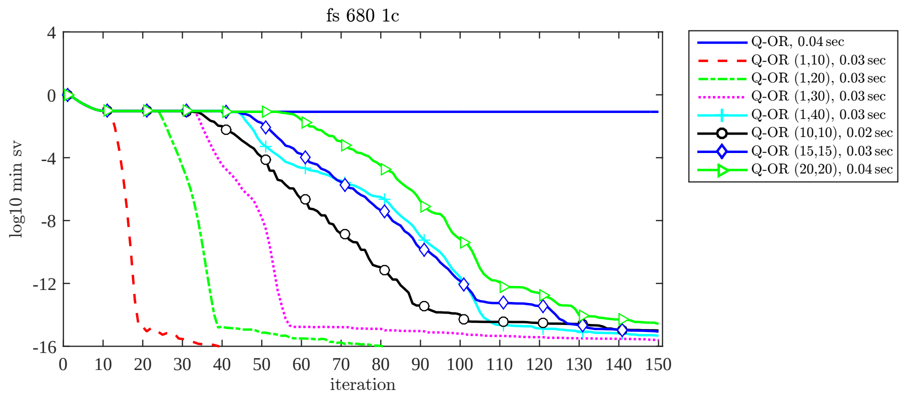

Fig. 4.28 fs 680 1c, $\log_{10}$ of minimum singular value of $V_{n,k}$, different values of (p,q)

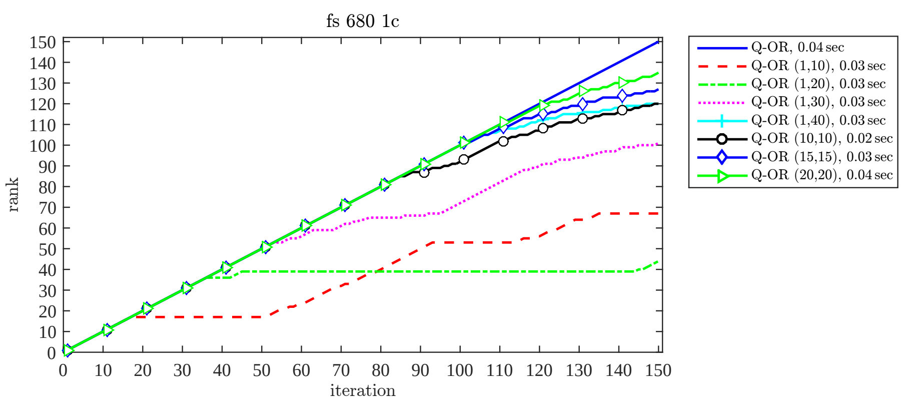

Fig. 4.29 fs 680 1c, numerical rank of $V_{n,k}$, different values of (p,q)

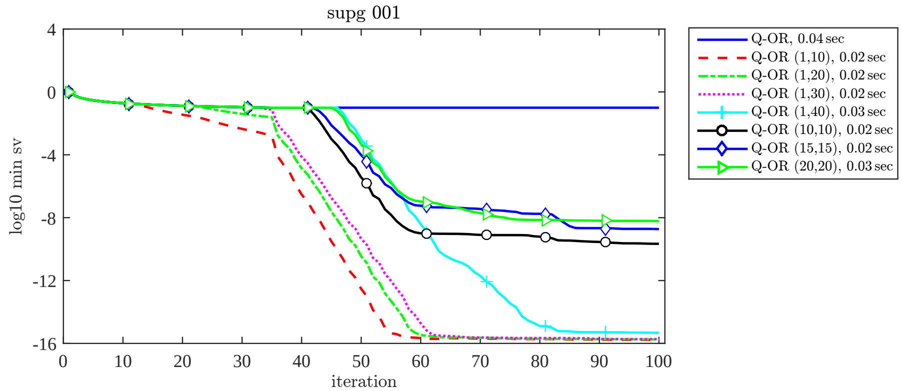

Fig. 4.30 supg 001, $\log_{10}$ of minimum singular value of $V_{n,k}$, different values of (p, q)

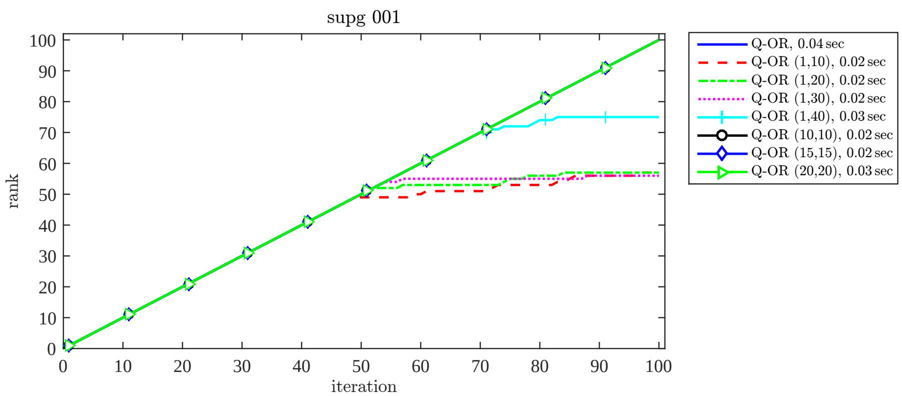

Fig. 4.31 supg 001, numerical rank of $V_{n,k}$, different values of (p, q)

Chapter 5
FOM/GMRES and variants

5.1 Introduction to FOM and GMRES

5.2 Convergence of FOM and GMRES

5.3 Prescribed convergence

5.4 Stagnation of GMRES

5.5 Residual norms

5.6 The residual polynomials

5.7 Study of convergence using unitary matrices

5.8 Estimates of the norm of the error

5.9 Other implementations of GMRES

5.10 Parallel computing

5.11 Finite precision arithmetic

5.12 Numerical examples

5.12.1 FOM and GMRES

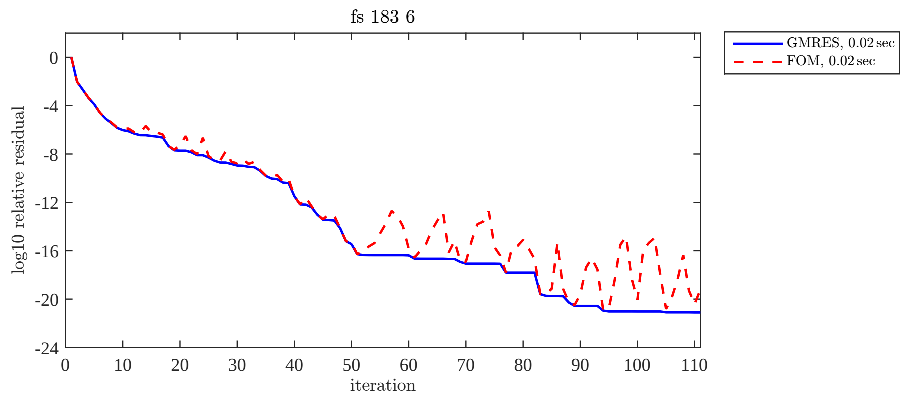

Fig. 5.1 `fs 183 6`, $\log_{10}$ of the relative residual norm, GMRES (plain) and FOM (dashed)

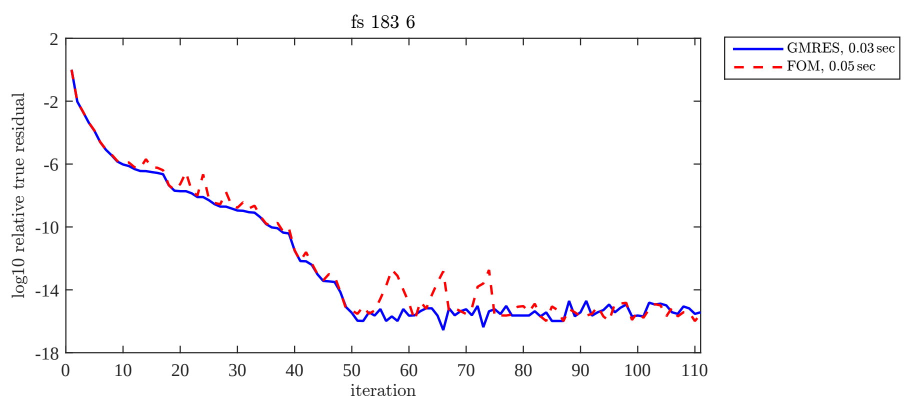

Fig. 5.2 `fs 183 6`, $\log_{10}$ of the relative true residual norm, GMRES (plain) and FOM (dashed)

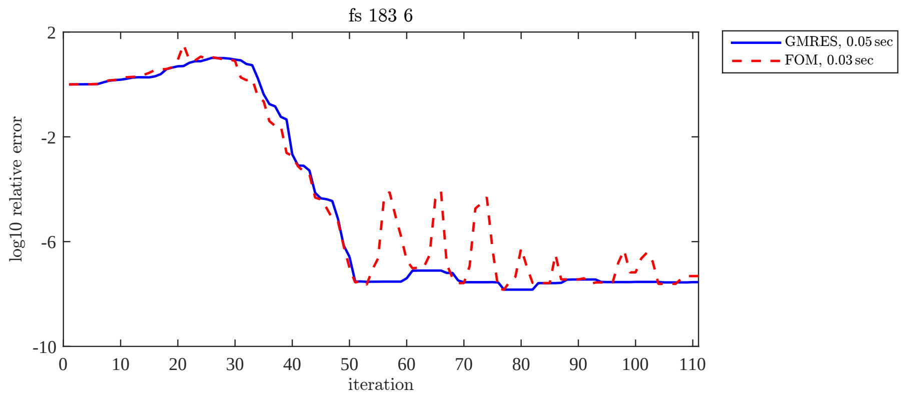

Fig. 5.3 `fs 183 6`, $\log_{10}$ of the relative error norm, GMRES (plain) and FOM (dashed)

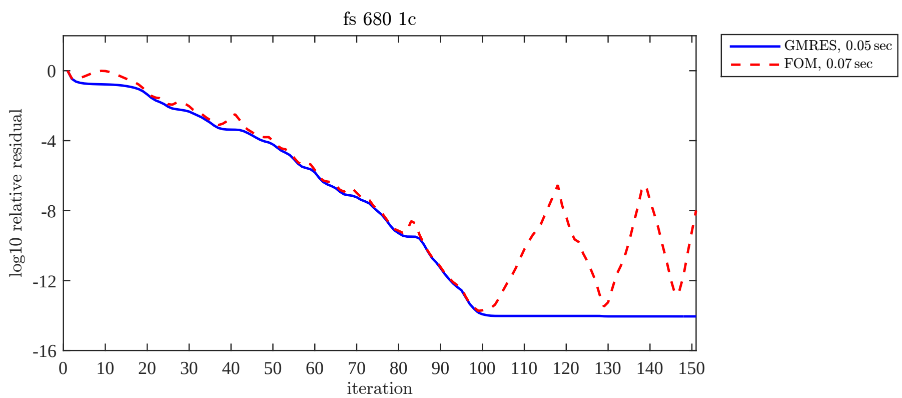

Fig. 5.4 `fs 680 1c`, $\log_{10}$ of the relative residual norm, GMRES (plain) and FOM (dashed)

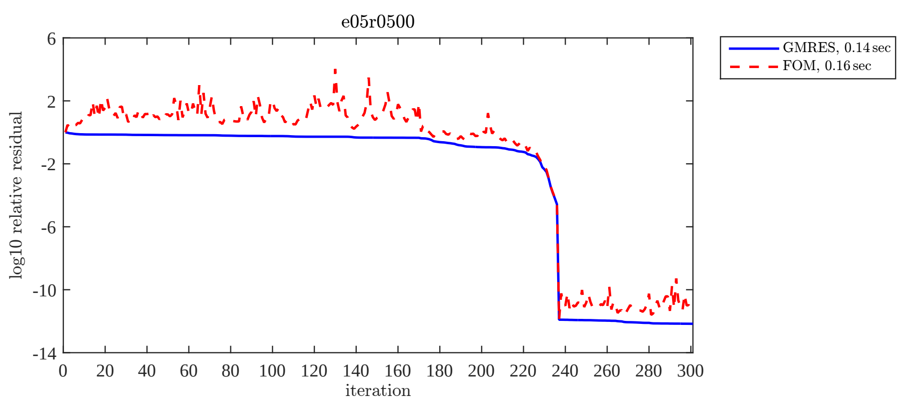

Fig. 5.5 `e05r0500`, $\log_{10}$ of the relative residual norm, GMRES (plain) and FOM (dashed)

5.12.2 Variants of GMRES

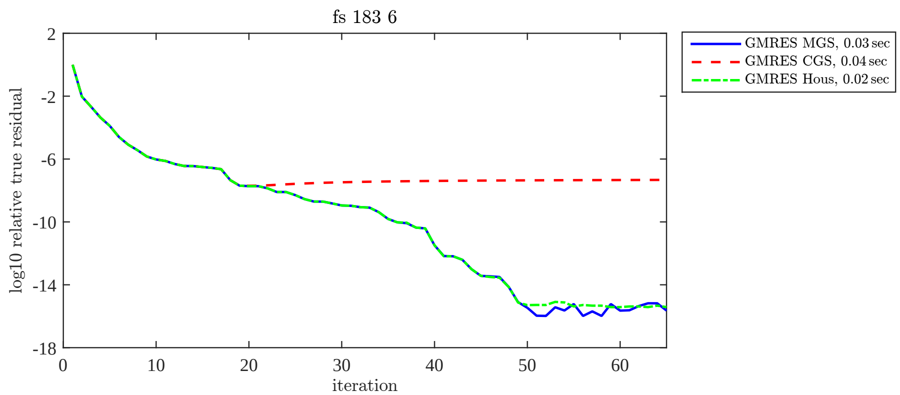

Fig. 5.6 `fs 183 6`, $\log_{10}$ of the relative true residual norm, GMRES, MGS (plain), CGS (dashed) and Householder (dot-dashed)

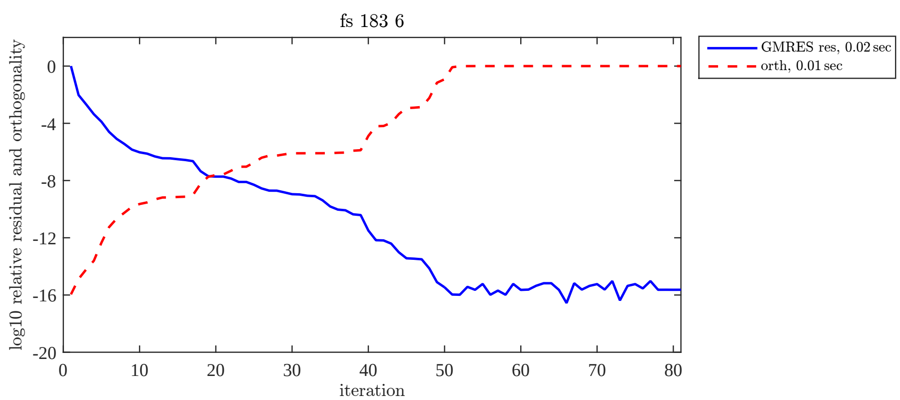

Fig. 5.7 `fs 183 6`, $\log_{10}$ of the relative true residual norm, GMRES-MGS (plain) and level of orthogonality(dashed)

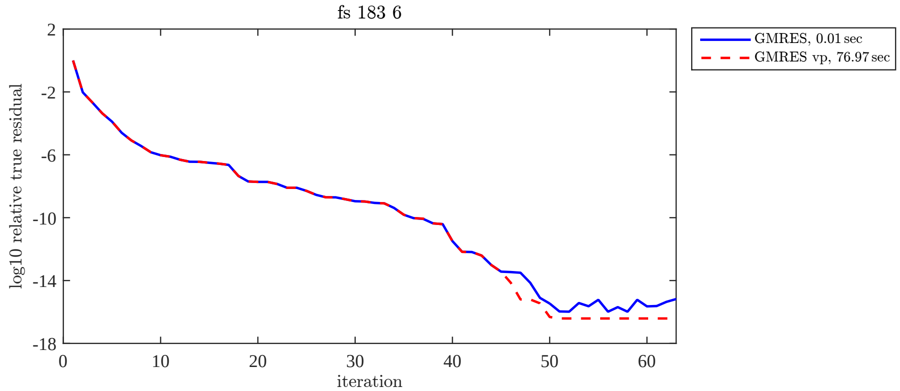

Fig. 5.8 `fs 183 6`, $\log_{10}$ of the relative true residual norm, GMRES-MGS double-precision (plain) and GMRES-MGS variable precision with 64 decimal digits (dashed)

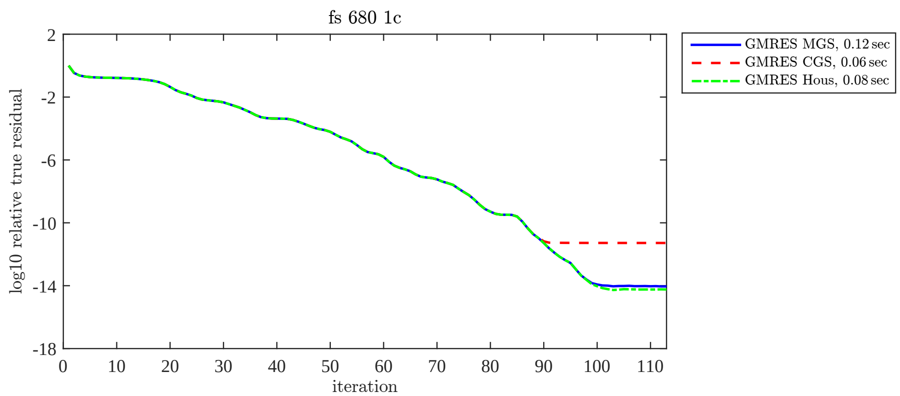

Fig. 5.9 `fs 680 1c`, $\log_{10}$ of the relative true residual norm, GMRES, MGS (plain), CGS (dashed) and Householder (dot-dashed)

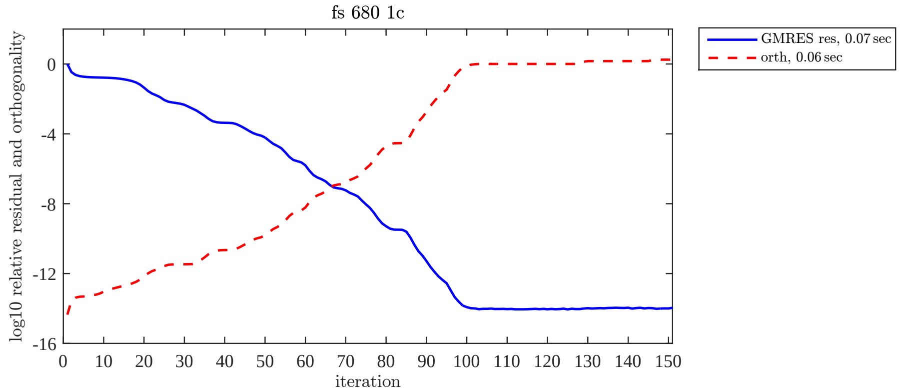

Fig. 5.10 `fs 680 1c`, $\log_{10}$ of the relative true residual norm, GMRES-MGS (plain) and level of orthogonality(dashed)

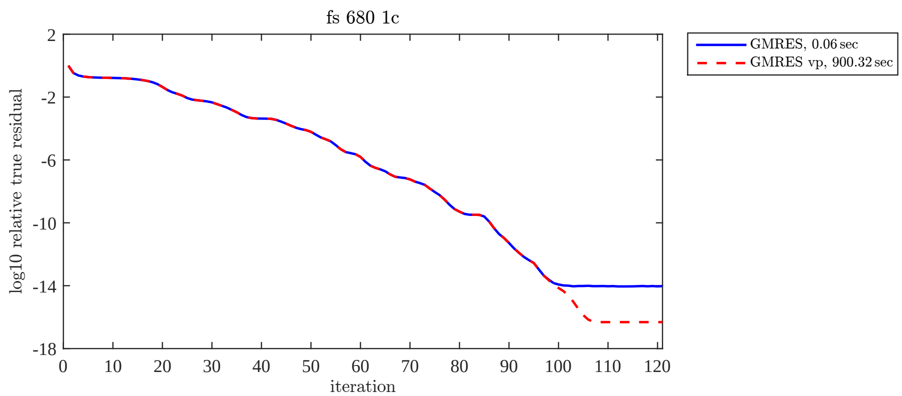

Fig. 5.11 `fs 680 1c`, $\log_{10}$ of the relative true residual norm, GMRES-MGS double-precision (plain) and GMRES-MGS variable precision with 64 decimal digits (dashed)

5.12.3 Prescribed convergence and stagnation

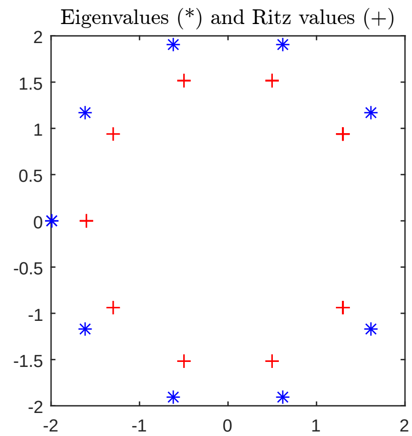

Fig. 5.12 Eigenvalues of A and Ritz values

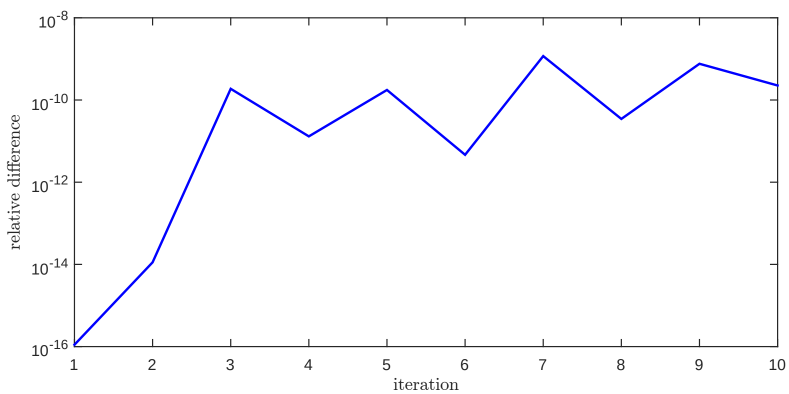

Fig. 5.13 Relative difference between the prescribed values g_k and the GMRES true generated residual norms

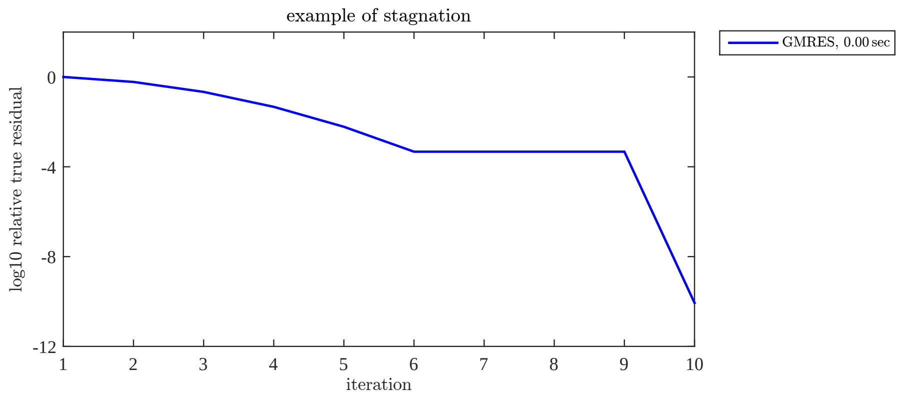

Fig. 5.14 GMRES-MGS true residual norms

5.12.4 Residual norm bounds

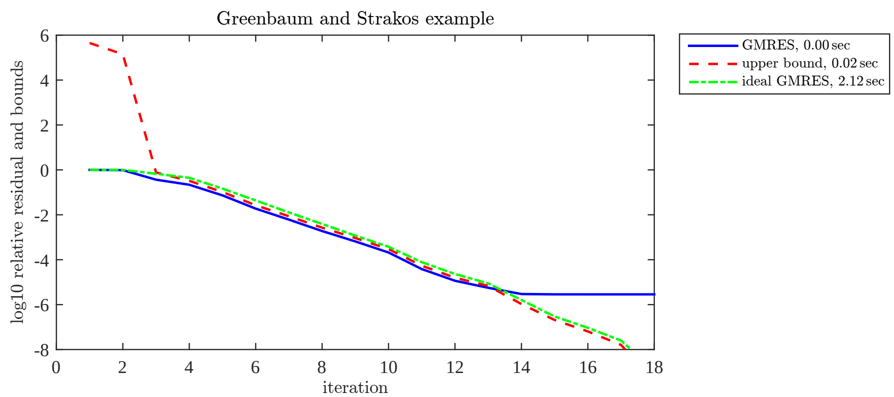

Fig. 5.15 Example from [?], GMRES-MGS true residual norms and bound (??)

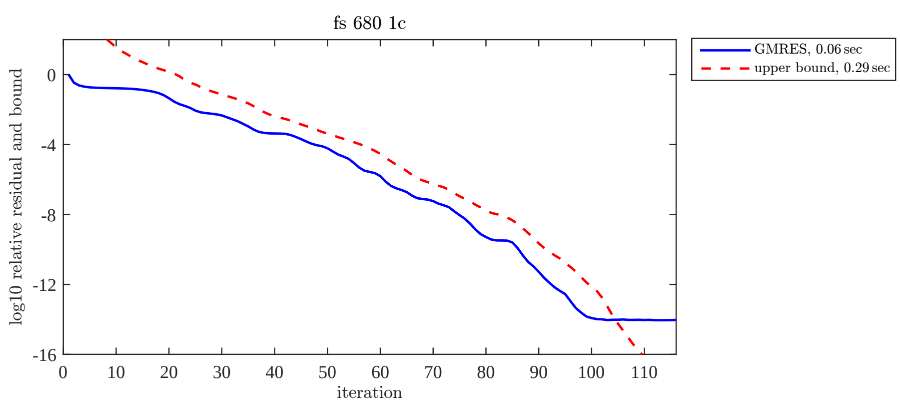

Fig. 5.16 `fs 680 1c`, GMRES-MGS true residual norms and bound

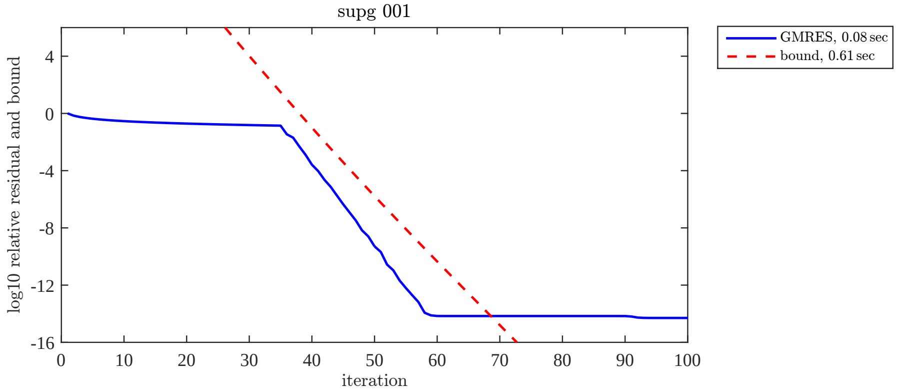

Fig. 5.17 `supg 001`, $n = 1225$, GMRES-MGS true residual norms and bound

5.12.5 Error norm estimates

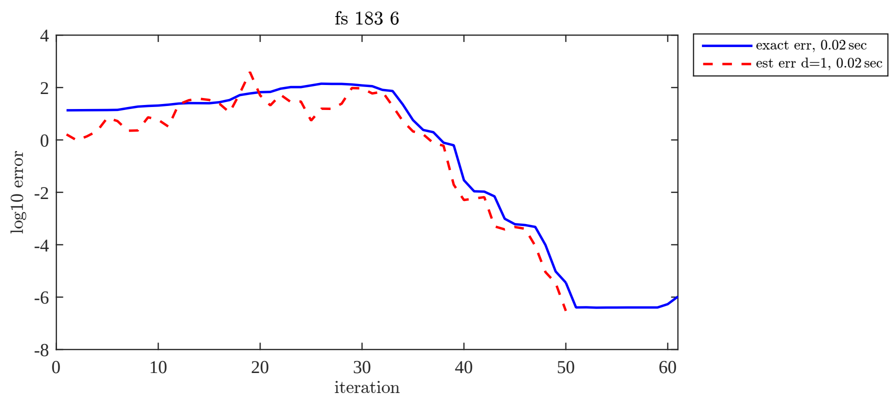

Fig. 5.18 `fs 183 6`, GMRES-MGS, exact error norm (plain) and estimate, $d = 1$ (dashed)

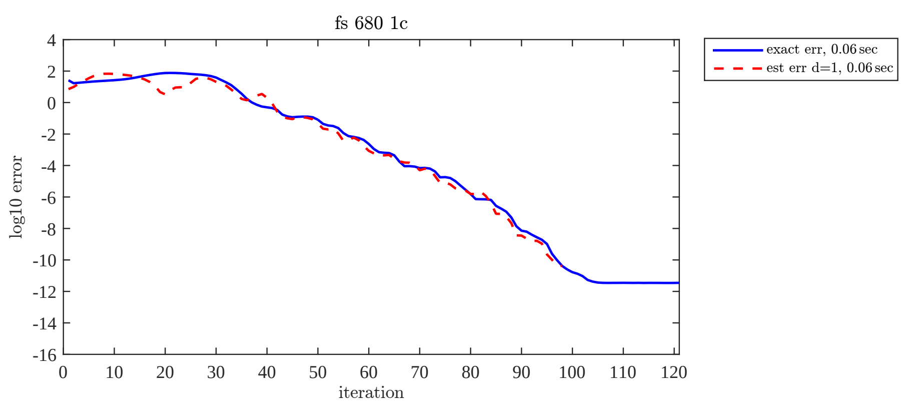

Fig. 5.19 `fs 680 1c`, GMRES-MGS, exact error norm (plain) and estimate, $d = 1$ (dashed)

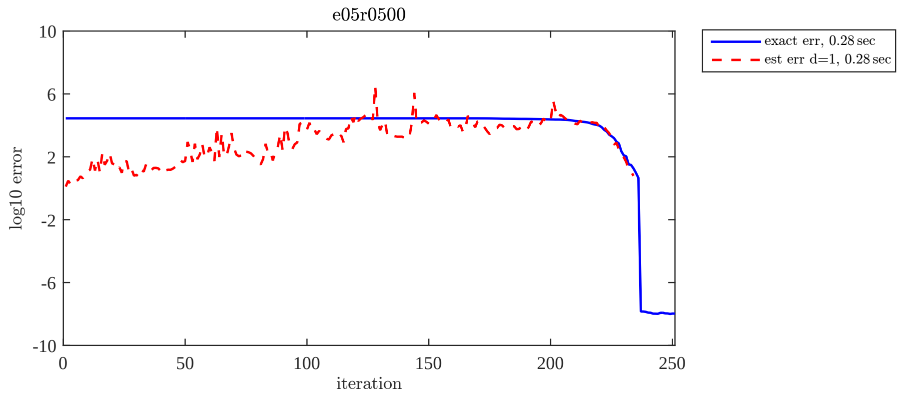

Fig. 5.20 `e05r0500`, GMRES-MGS, exact error norm (plain) and estimate, $d = 1$ (dashed)

Chapter 6
Methods equivalent to FOM or GMRES

6.1 GCR, Orthomin, Orthodir and Axelsson's method

6.2 Simpler, residual-based simpler and adaptive simpler GMRES

6.3 Orthores

6.4 Q-OR Optinv

6.5 Parallel computing

6.6 Finite precision arithmetic

6.7 Numerical examples

6.7.1 GCR, Orthodir and Axelsson

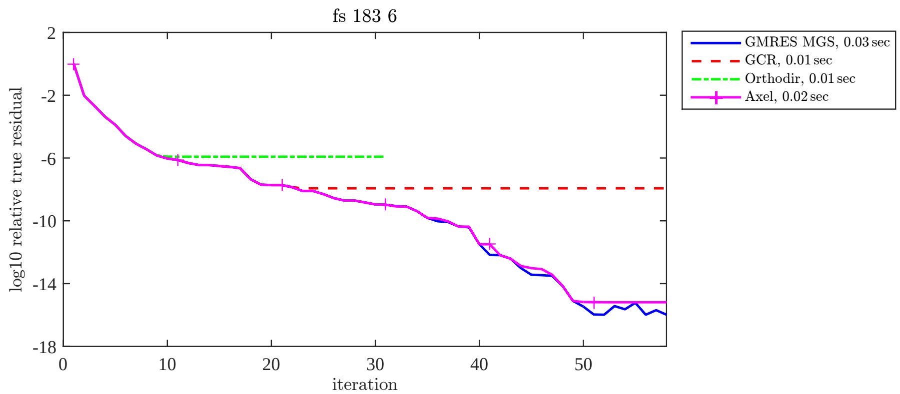

Fig. 6.1 `fs 183 6`, true residual norms, GMRES-MGS (plain), GCR (dashed), Orthodir (dot-dashed), Axelsson (+)

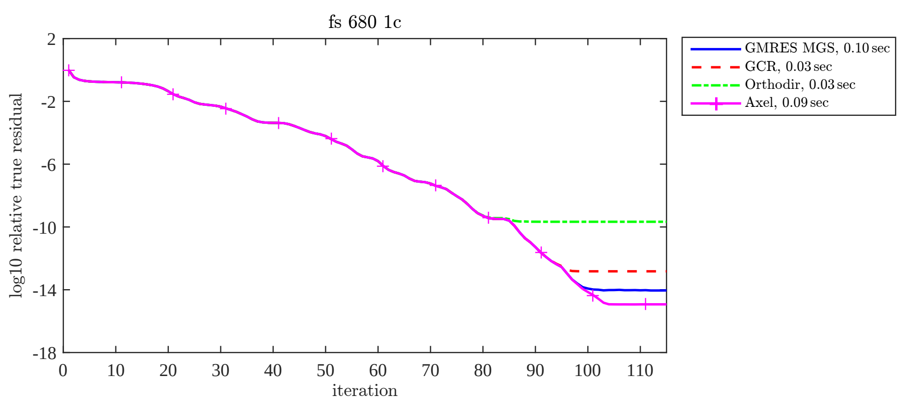

Fig. 6.2 `fs 680 1c`, true residual norms, GMRES-MGS (plain), GCR (dashed), Orthodir (dot-dashed), Axelsson (+)

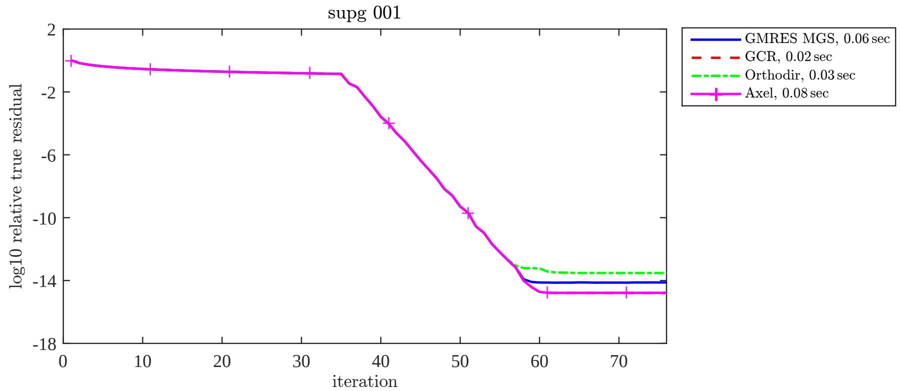

Fig. 6.3 `supg 001`, true residual norms, GMRES-MGS (plain), GCR (dashed), Orthodir (dot-dashed), Axelsson (+)

6.7.2 ASGMRES

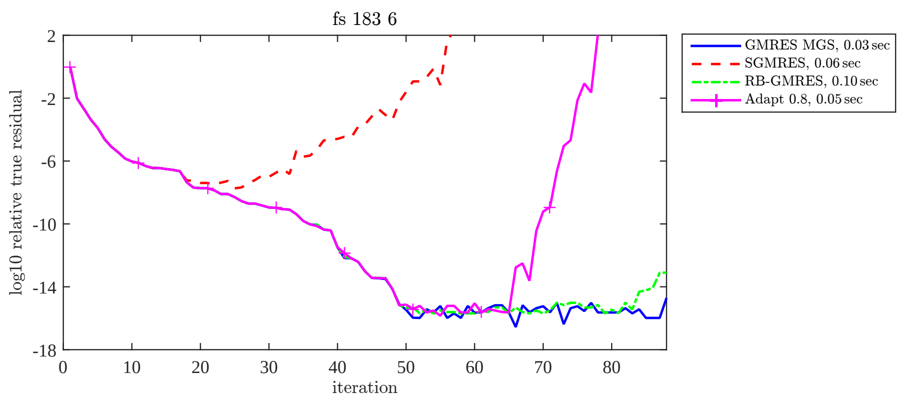

Fig. 6.4 `fs 183 6`, relative true residual norms, GMRES-MGS (plain), SGMRES (dashed), RB GMRES (dot-dashed), ASGMRES $\nu = 0.8$ (+)

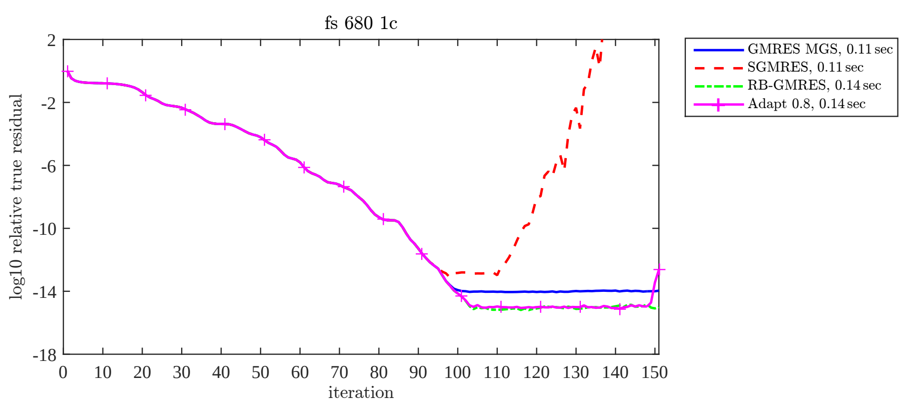

Fig. 6.5 `fs 680 1c`, relative true residual norms, GMRES-MGS (plain), SGMRES (dashed), RB GMRES (dot-dashed), ASGMRES $\nu = 0.8$ (+)

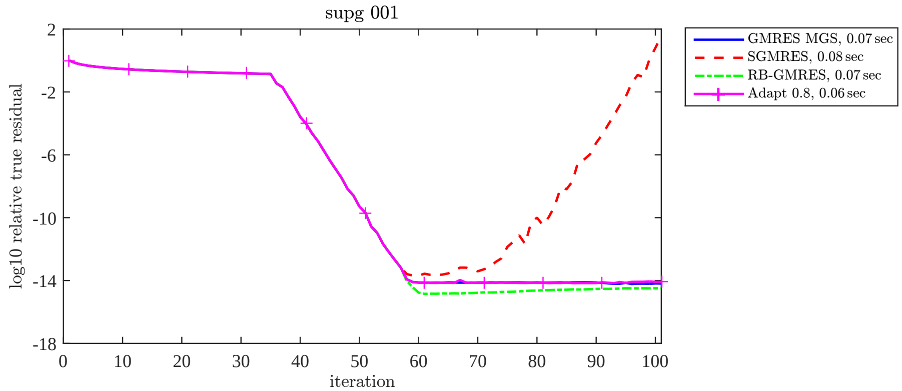

Fig. 6.6 `supg 001`, relative true residual norms, GMRES-MGS (plain), SGMRES (dashed), RB GMRES (dot-dashed), ASGMRES $\nu = 0.8$ (+)

6.7.3 FOM and Orthores

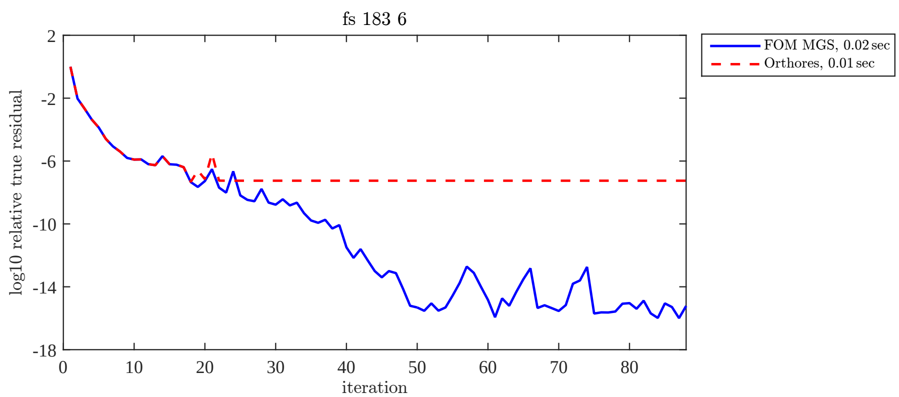

Fig. 6.7 `fs 183 6`, relative true residual norms, FOM-MGS (plain), Orthores (dashed)

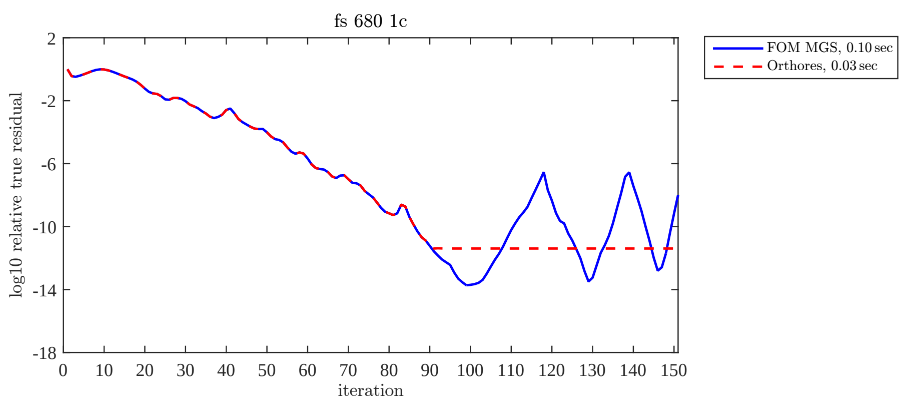

Fig. 6.8 `fs 680 1c`, relative true residual norms, FOM-MGS (plain), Orthores (dashed)

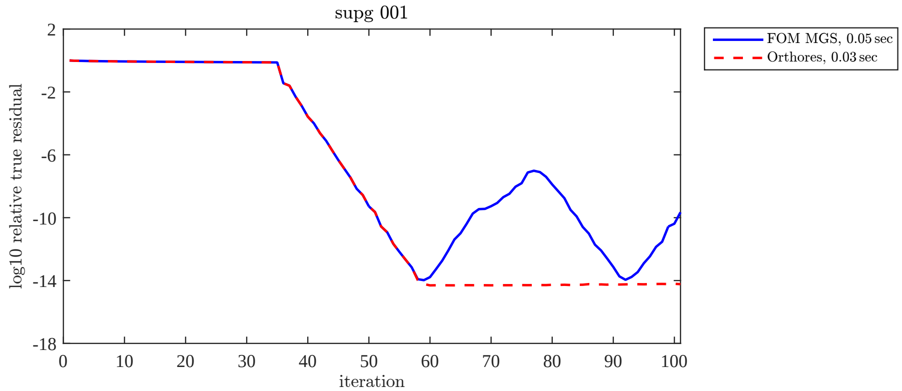

Fig. 6.9 `supg 001`, order 1225, relative true residual norms, FOM-MGS (plain), Orthores (dashed)

6.7.4 Q-OR Optinv

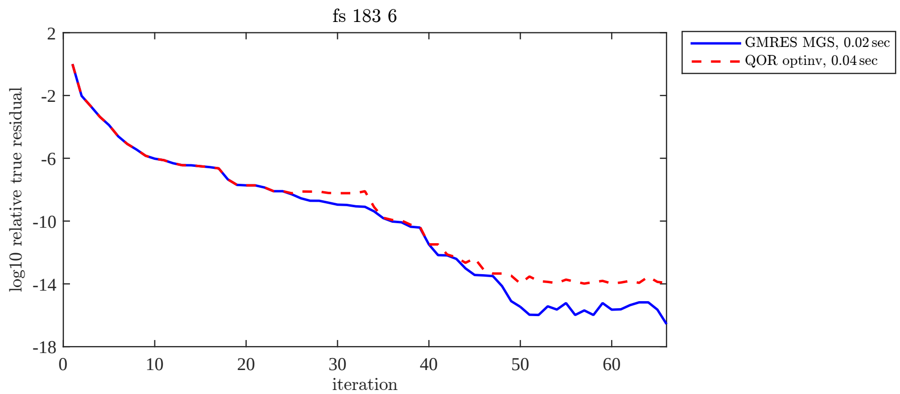

Fig. 6.10 `fs 183 6`, relative true residual norms, GMRES-MGS (plain), Q-OR Optinv (dashed)

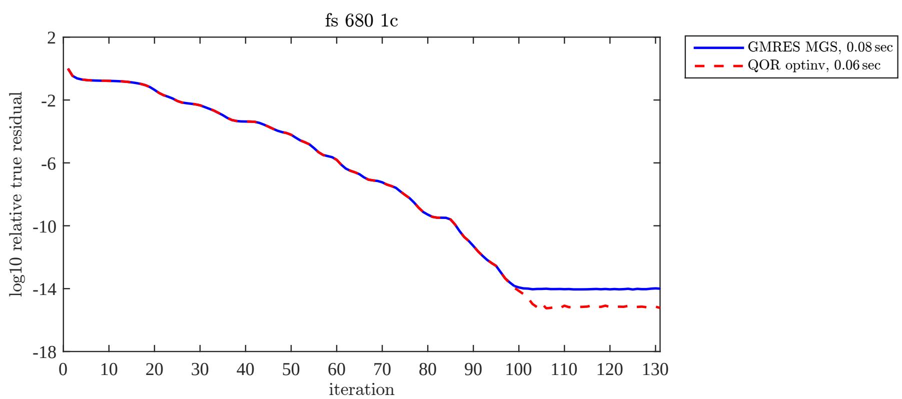

Fig. 6.11 `fs 680 1c`, relative true residual norms, GMRES-MGS (plain), Q-OR Optinv (dashed)

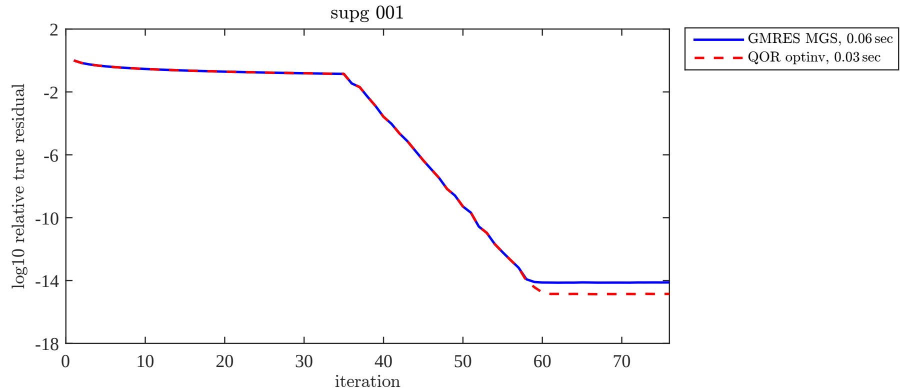

Fig. 6.12 `supg 001`, order 1225, relative true residual norms, GMRES-MGS (plain), Q-OR Optinv (dashed)

Chapter 7
Hessenberg/CMRH

7.1 Derivation of the methods

7.2 Comparison with GMRES and convergence of CMRH

7.3 Prescribed convergence

7.4 Stagnation of CMRH

7.5 Residual norms

7.6 Parallel computing

7.7 Finite precision arithmetic

7.8 Numerical experiments

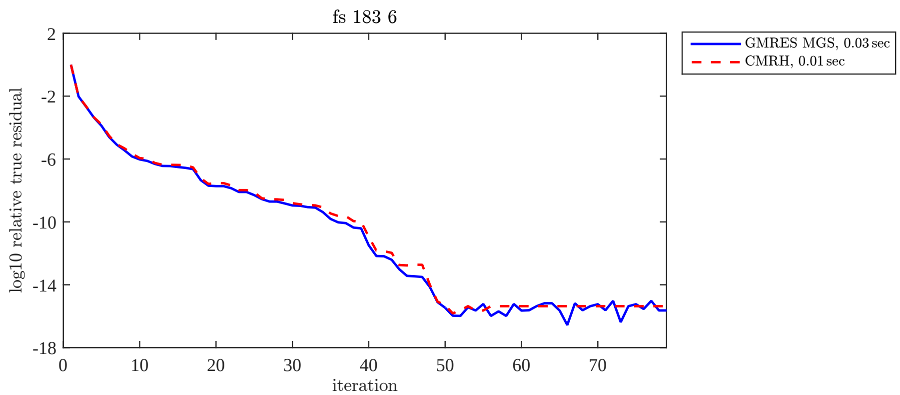

Fig. 7.1 `fs 183 6`, relative true residual norms, GMRES-MGS (plain), CMRH (dashed)

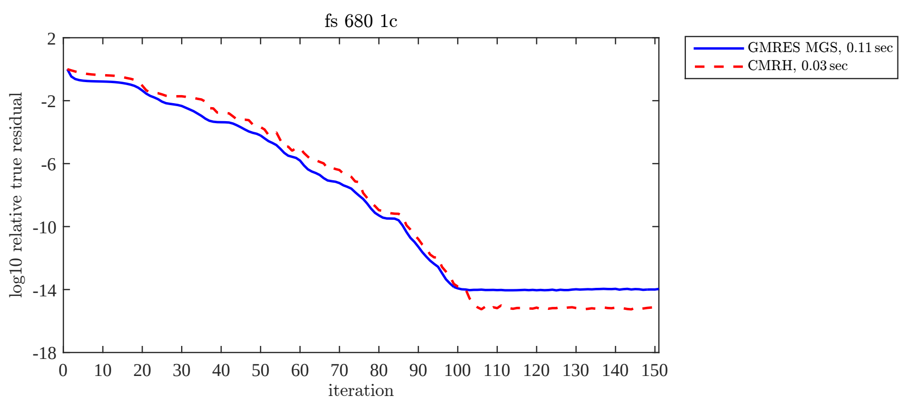

Fig. 7.2 `fs 680 1c`, relative true residual norms, GMRES-MGS (plain), CMRH (dashed)

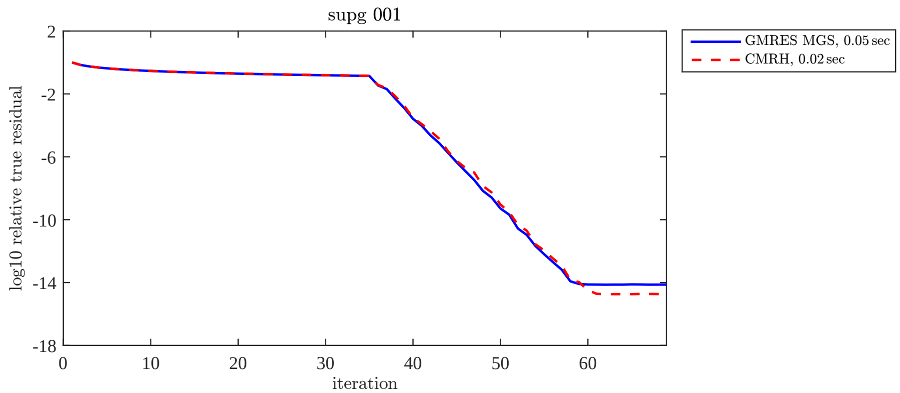

Fig. 7.3 `supg 001`, order 1225, relative true residual norms, GMRES-MGS (plain), CMRH (dashed)

Chapter 8
BiCG/QMR and Lanczos algorithms

8.1 The Lanczos algorithms

8.2 Derivation of BiCG

8.3 QMR

8.4 Breakdowns and look-ahead in BiCG/QMR

8.5 Comparison of QMR and GMRES

8.6 Prescribed convergence in BiCG and QMR

8.7 Residual norms

8.8 Lanczos algorithms with look-ahead and formal orthogonal polynomials

8.9 Parallel computing

8.10 Finite precision arithmetic

8.11 Numerical examples

8.11.1 BiCG

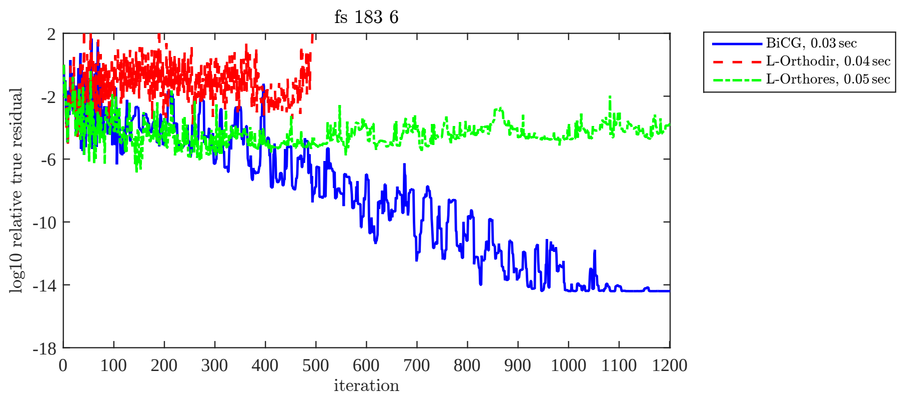

Fig. 8.1 `fs 183 6`, relative true residual norms, BiCG (plain), Lanczos-Orthodir (dashed), Lanczos-Orthores (dot-dashed)

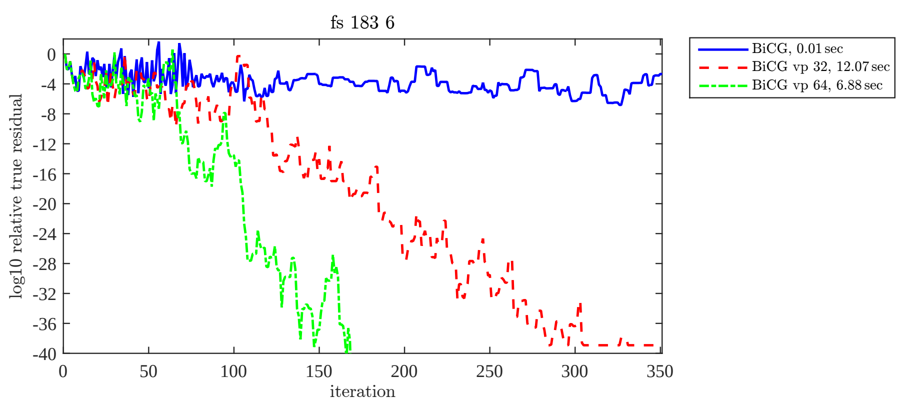

Fig. 8.2 `fs 183 6`, $\log_{10}$ of the relative true residual norm, BiCG (plain), BiCG variable precision with 32 decimal digits (dashed) and with 64 decimal digits (dot-dashed)

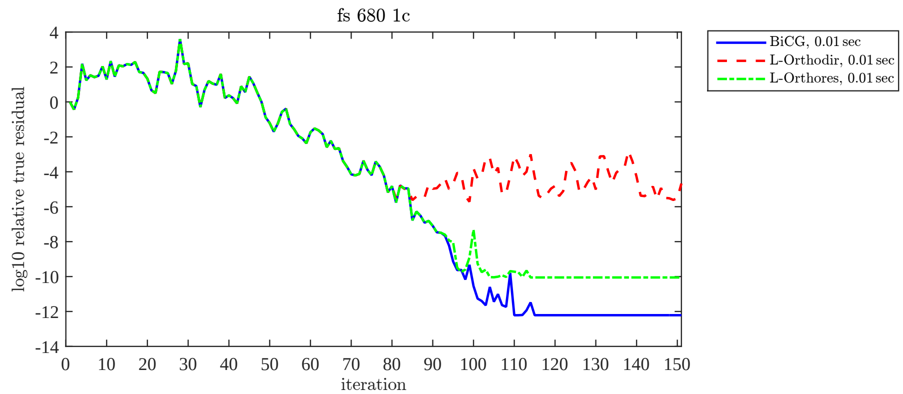

Fig. 8.3 `fs 680 1c`, relative true residual norms, BiCG (plain), Lanczos-Orthodir (dashed), Lanczos-Orthores (dot-dashed)

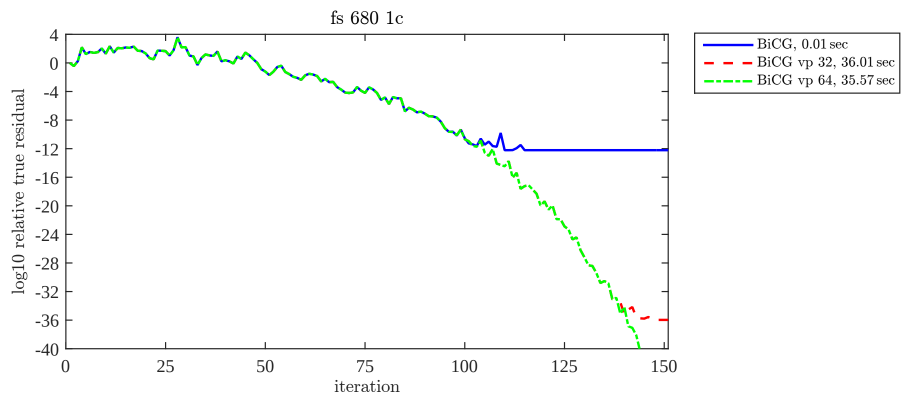

Fig. 8.4 `fs 680 1c`, $\log_{10}$ of the relative true residual norm, BiCG (plain), BiCG variable precision with 32 decimal digits (dashed) and with 64 decimal digits (dot-dashed)

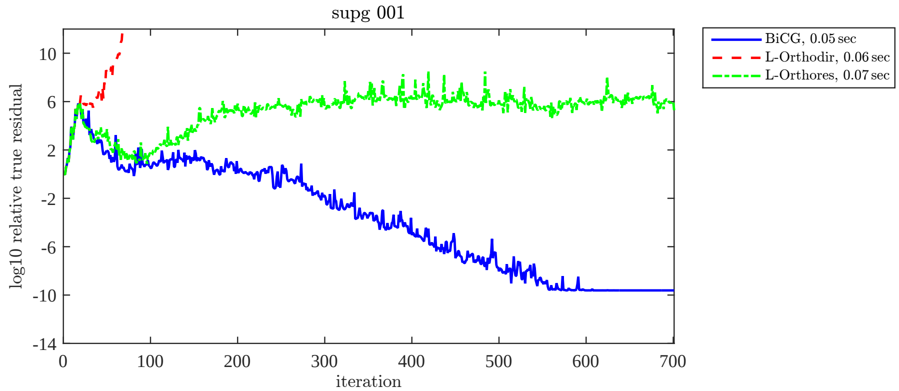

Fig. 8.5 `supg 001`, order 1225, relative true residual norms, BiCG (plain), Lanczos-Orthodir (dashed), Lanczos-Orthores (dot-dashed)

8.11.2 QMR

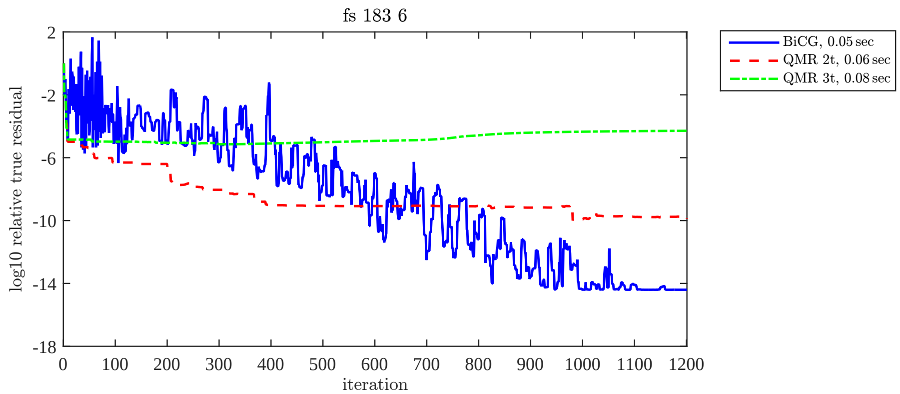

Fig. 8.6 `fs 183 6`, relative true residual norms, BiCG (plain), QMR 2t (dashed), QMR 3t (dot-dashed)

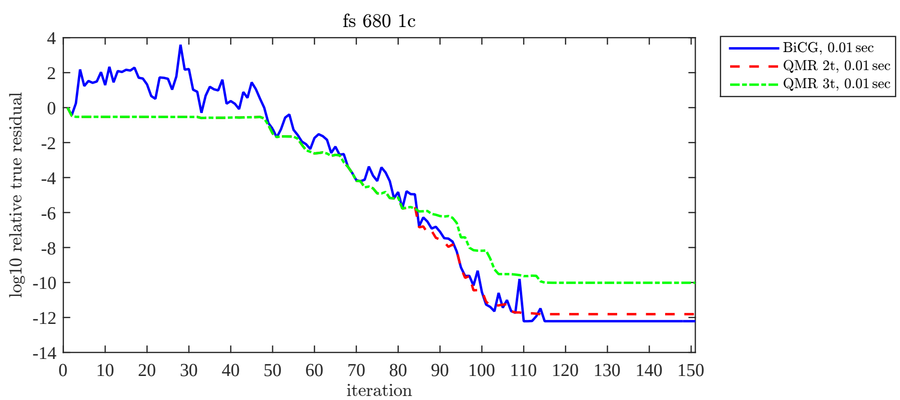

Fig. 8.7 `fs 680 1c`, relative true residual norms, BiCG (plain), QMR 2t (dashed), QMR 3t (dot-dashed)

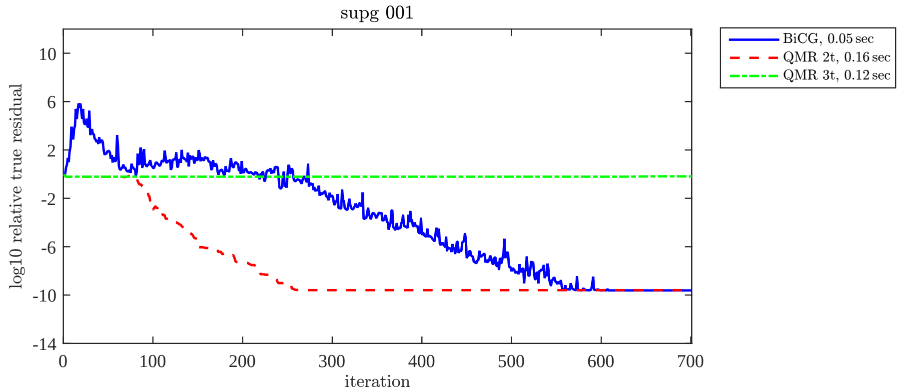

Fig. 8.8 `supg 001`, order 1225, relative true residual norms, BiCG (plain), QMR 2t (dashed), QMR 3t (dot-dashed)

8.11.3 Comparisons with GMRES

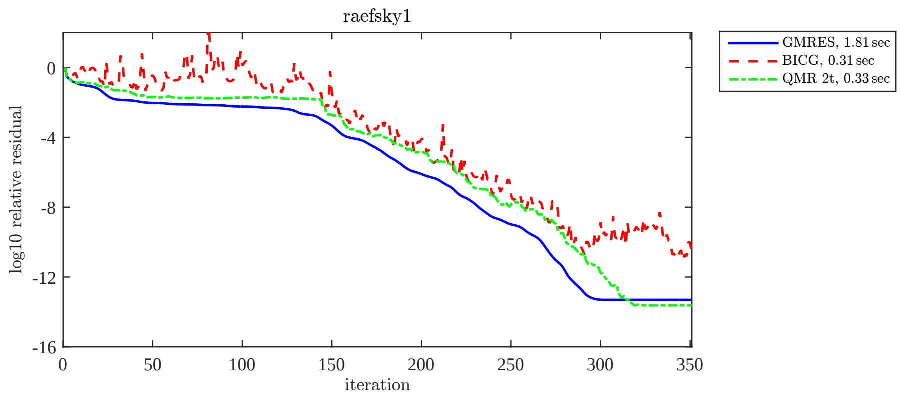

Fig. 8.9 `raefsky1`, relative residual norms versus iteration number, GMRES-MGS (plain), BiCG (dashed), QMR 2t (dot-dashed)

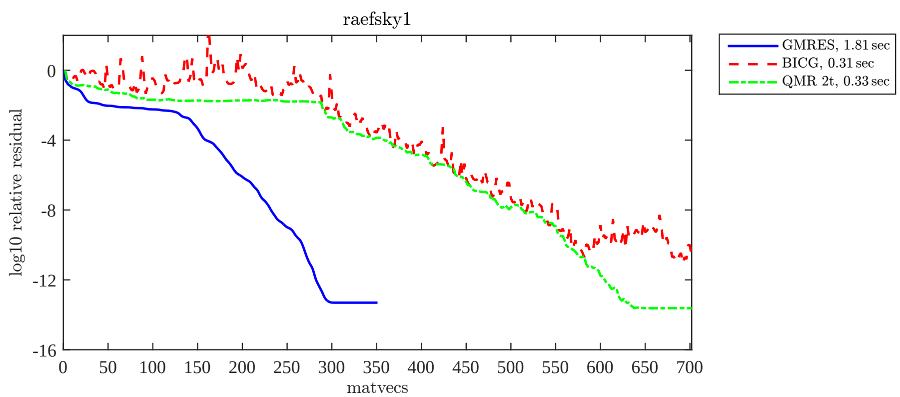

Fig. 8.10 `raefsky1`, relative residual norms versus number of matrix-vector products, GMRES-MGS (plain), BiCG (dashed), QMR 2t (dot-dashed)

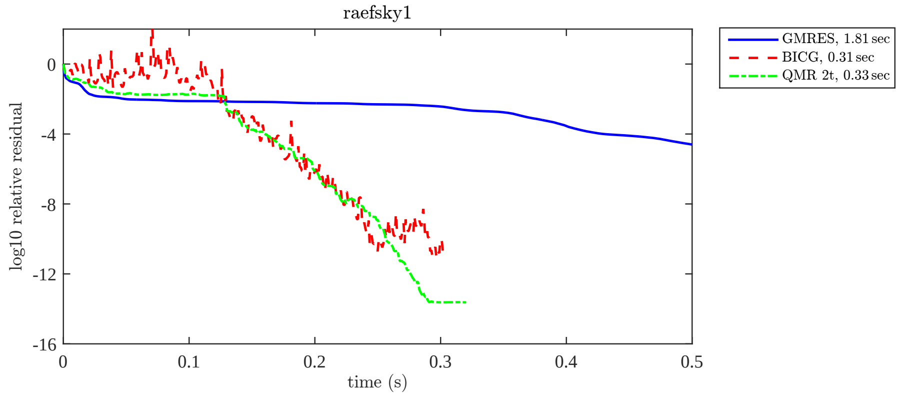

Fig. 8.11 `raefsky1`, relative residual norms versus computing time, GMRES-MGS (plain), BiCG (dashed), QMR 2t (dot-dashed)

8.11.4 Methods with look-ahead

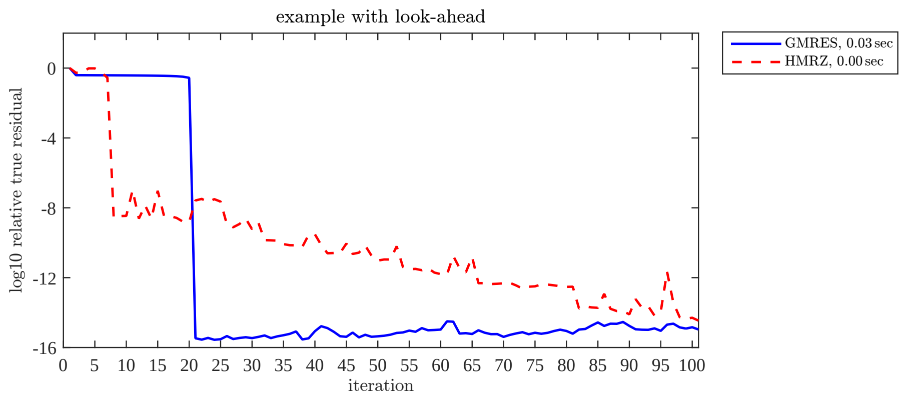

Fig. 8.12 Relative true residual norms, GMRES-MGS (plain), HMRZ-stab (dashed)

8.11.5 Ai/Bj

Chapter 9
Transpose-free Lanczos methods

9.1 CGS

9.2 BiCGStab and extensions

9.3 Other product-type methods

9.4 Look-ahead for transpose-free methods

9.5 Parallel computing

9.6 Finite precision arithmetic

9.7 Numerical experiments

9.7.1 BiCGS

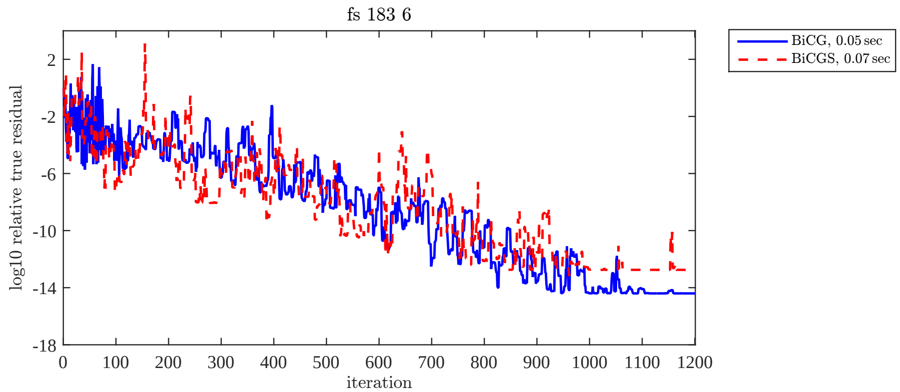

Fig. 9.1 `fs 183 6`, relative true residual norms, BiCG (plain), BiCGS (dashed)

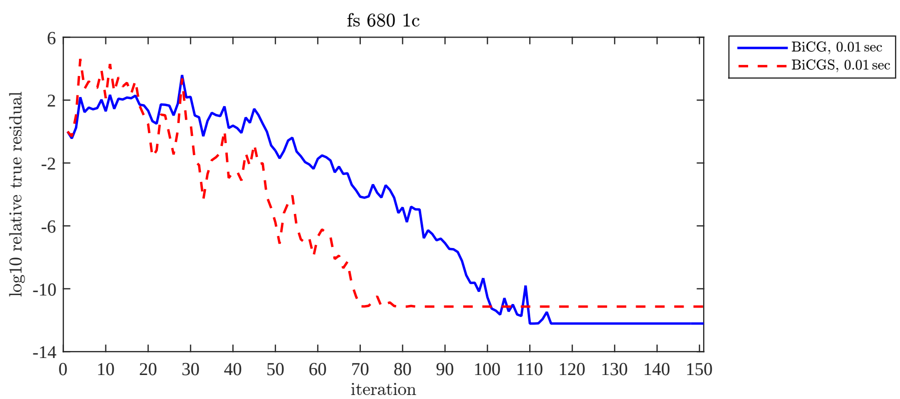

Fig. 9.2 `fs 680 1c`, relative true residual norms, BiCG (plain), BiCGS (dashed)

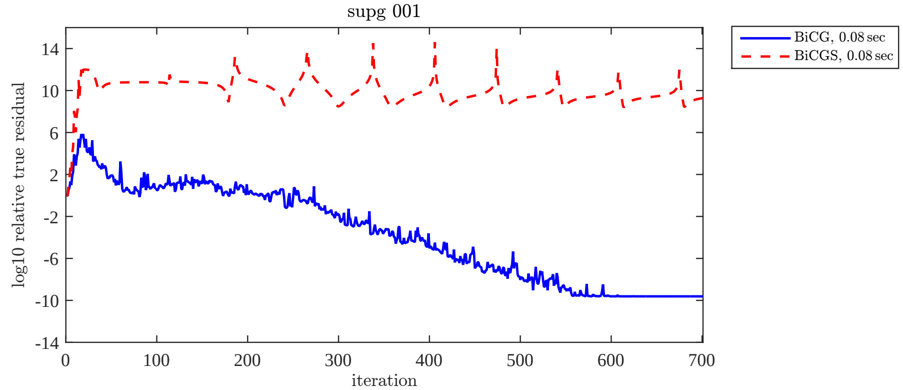

Fig. 9.3 `supg 001`, order 1225, relative true residual norms, BiCG (plain), BiCGS (dashed)

9.7.2 BiCGStab and variants

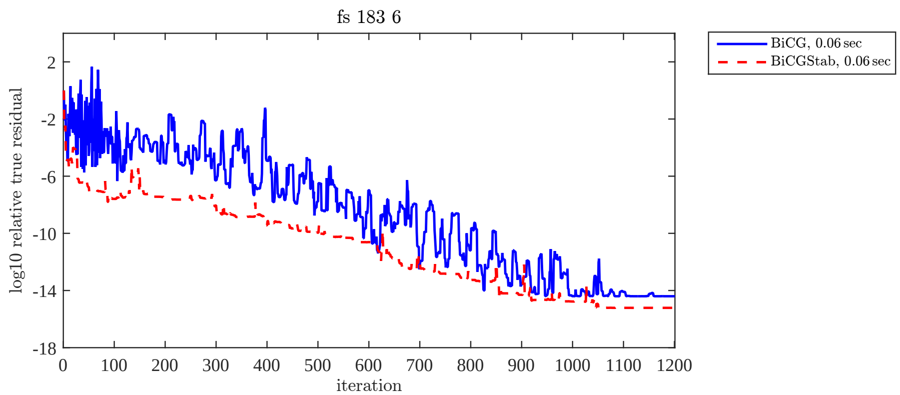

Fig. 9.4 `fs 183 6`, relative true residual norms, BiCG (plain), BiCGStab (dashed)

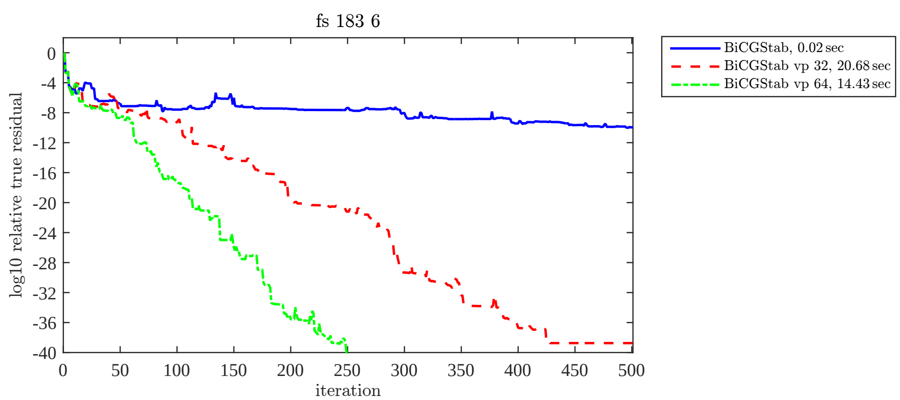

Fig. 9.5 `fs 183 6`, $\log_{10}$ of the relative true residual norm, BiCGStab (plain), BiCGStab variable precision with 32 decimal digits (dashed) and with 64 decimal digits (dot-dashed)

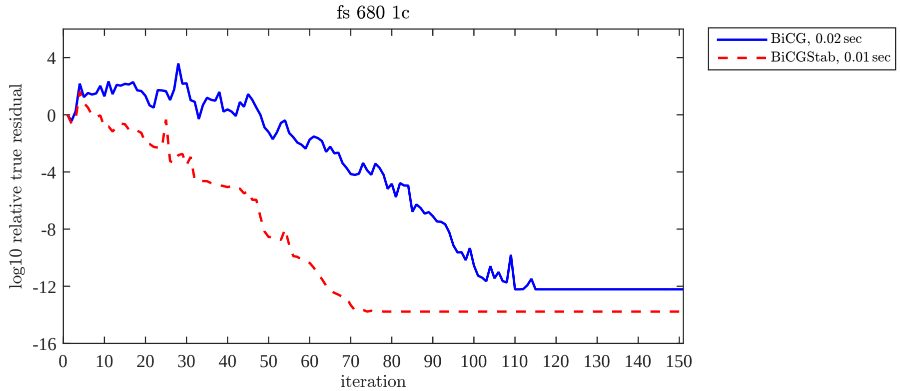

Fig. 9.6 `fs 680 1c`, relative true residual norms, BiCG (plain), BiCGStab (dashed)

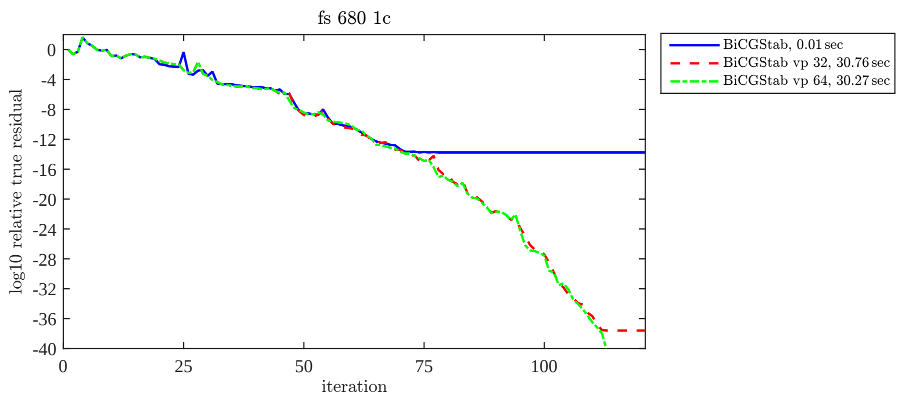

Fig. 9.7 `fs 680 1c`, $\log_{10}$ of the relative true residual norm, BiCGStab (plain), BiCGStab variable precision with 32 decimal digits (dashed) and with 64 decimal digits (dot-dashed)

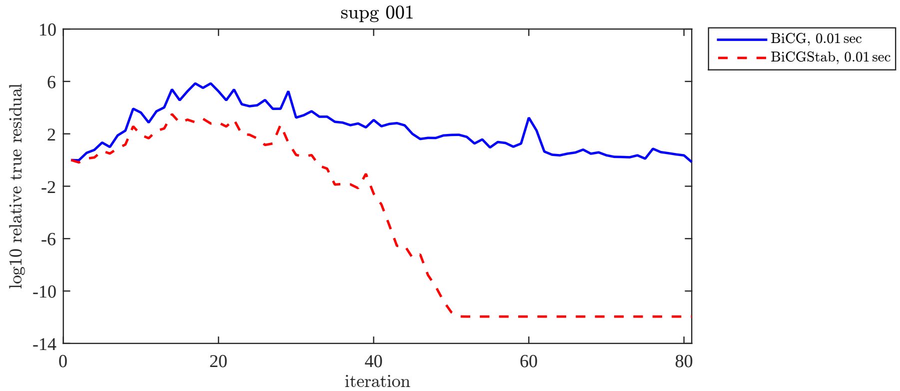

Fig. 9.8 `supg 001`, order 1225, relative true residual norms, BiCG (plain), BiCGStab (dashed)

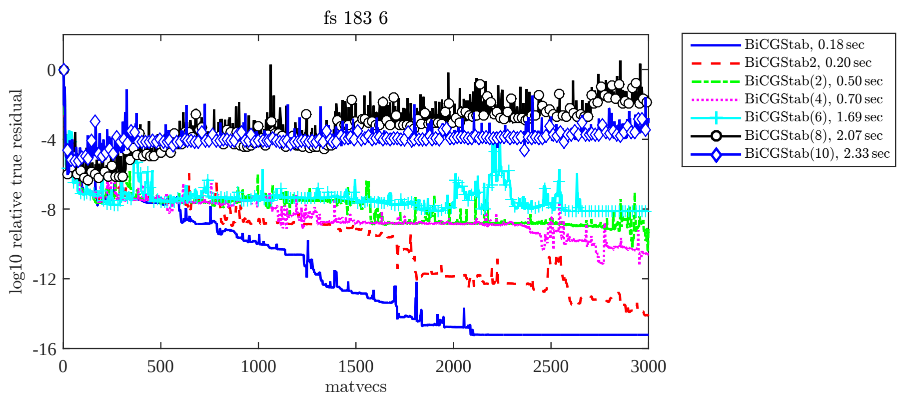

Fig. 9.9 `fs 183 6`, relative true residual norms, BiCGStab (plain), BiCGStab2 (dashed), BiCGtab(ℓ) $\ell = 2 : 2 : 10$

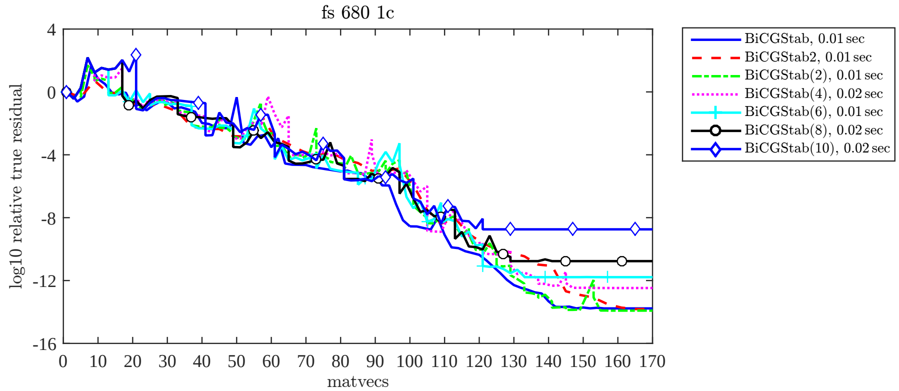

Fig. 9.10 `fs 680 1c`, relative true residual norms, BiCGStab (plain), BiCGStab2 (dashed), BiCGtab(ℓ) $\ell = 2:2:10$

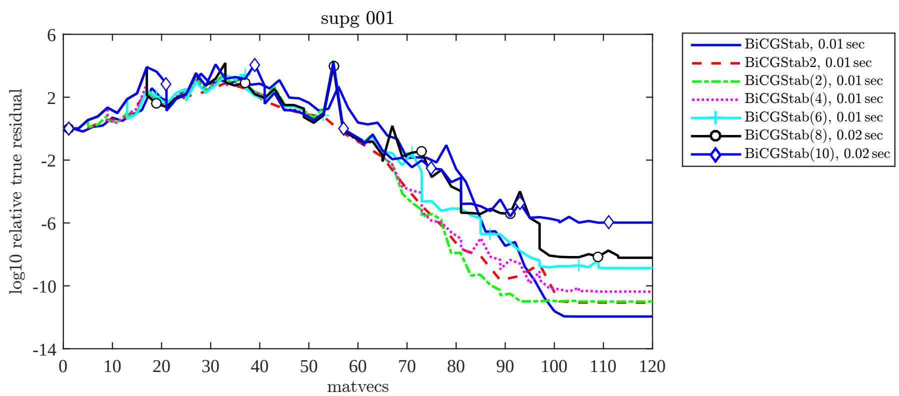

Fig. 9.11 `supg 001`, order 1225, relative true residual norms, BiCGStab (plain), BiCGStab2 (dashed), BiCGtab(ℓ) $\ell = 2:2:10$

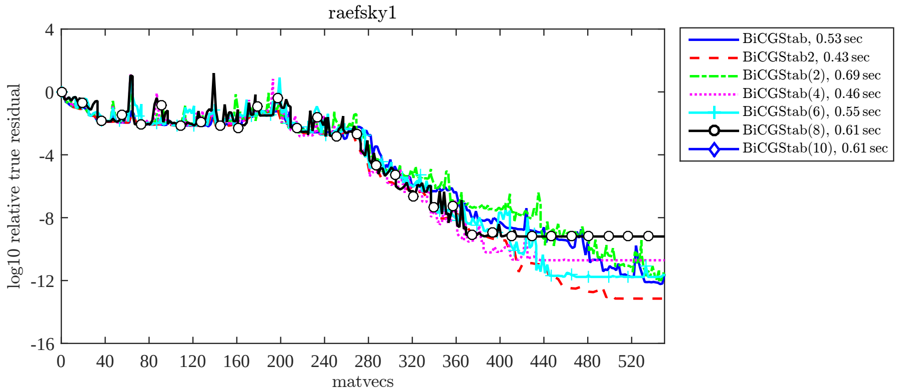

Fig. 9.12 `raefsky1`, relative true residual norms, BiCGStab (plain), BiCGStab2 (dashed), BiCGtab(ℓ) $\ell = 2:2:10$

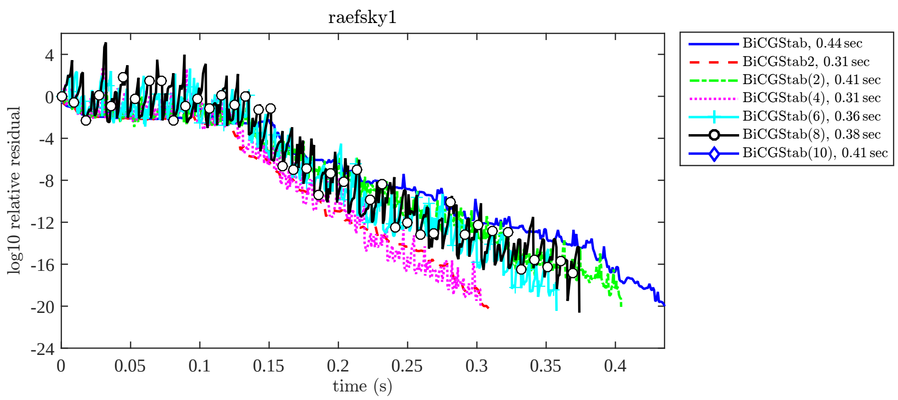

Fig. 9.13 `raefsky1`, relative residual norms, BiCGStab (plain), BiCGStab2 (dashed), BiCGtab(ℓ) $\ell = 2:2:10$

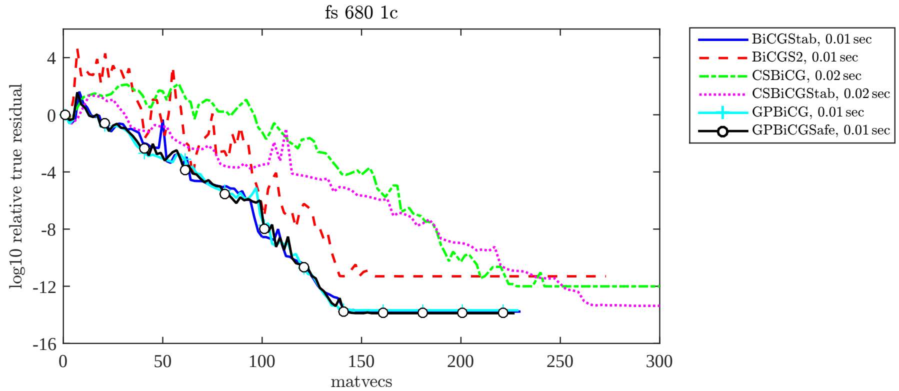

Fig. 9.14 `fs 680 1c`, relative true residual norms, different BiCG-like algorithms

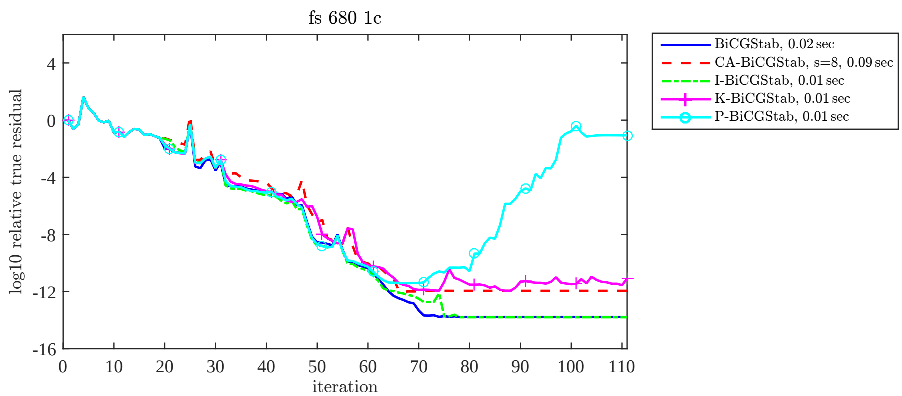

Fig. 9.15 `fs 680 1c`, relative true residual norms, BiCGStab (plain), CA-BiCGStab (dashed), I-BiCGtab (dot-dashed), K-BiCGStab (+), P-BiCGStab (o)

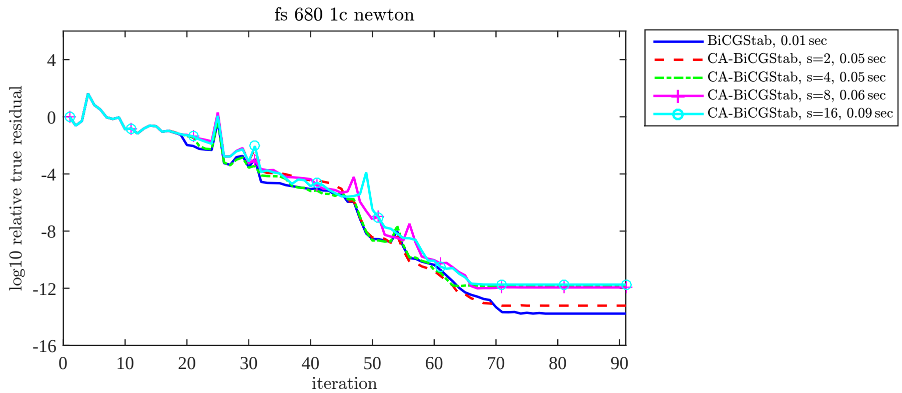

Fig. 9.16 `fs 680 1c`, relative true residual norms, BiCGStab (plain), CA-BiCGStab $s = 2$ (dashed), $s = 4$ (dot-dashed), $s = 8$ (+), $s = 16$ (o)

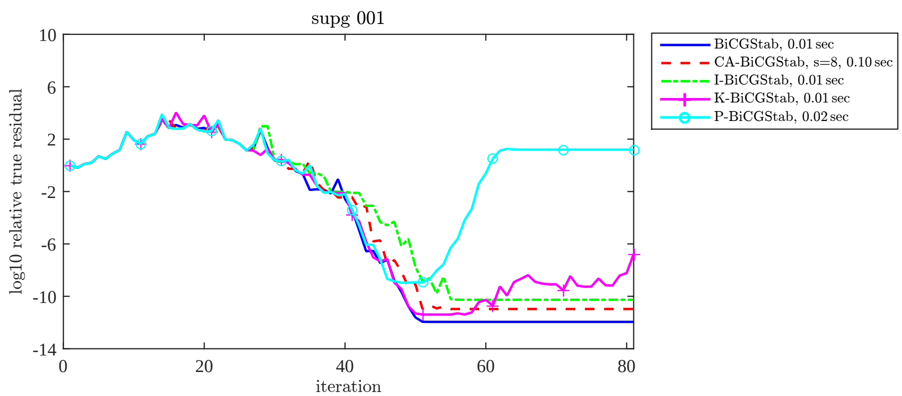

Fig. 9.17 `supg 001`, order 1225, relative true residual norms, BiCGStab (plain), CA-BiCGStab (dashed), I-BiCGtab (dot-dashed), K-BiCGStab (+), P-BiCGStab (o)

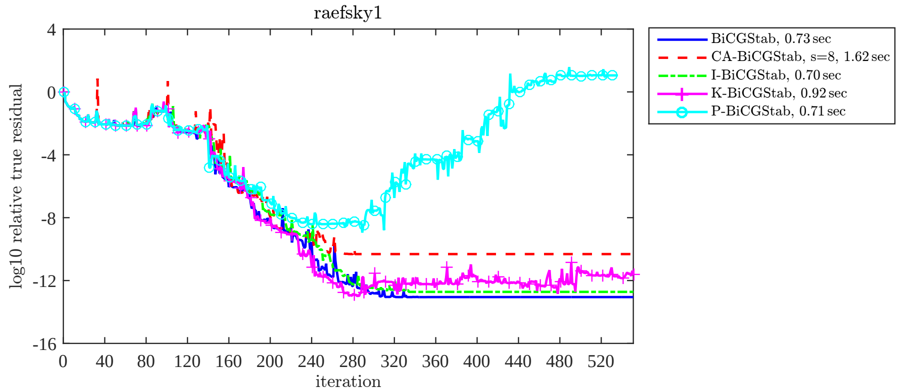

Fig. 9.18 `raefsky1`, relative true residual norms, BiCGStab (plain), CA-BiCGStab (dashed), I-BiCGtab (dot-dashed), K-BiCGStab (+), P-BiCGStab (o)

9.7.3 QMR-like methods

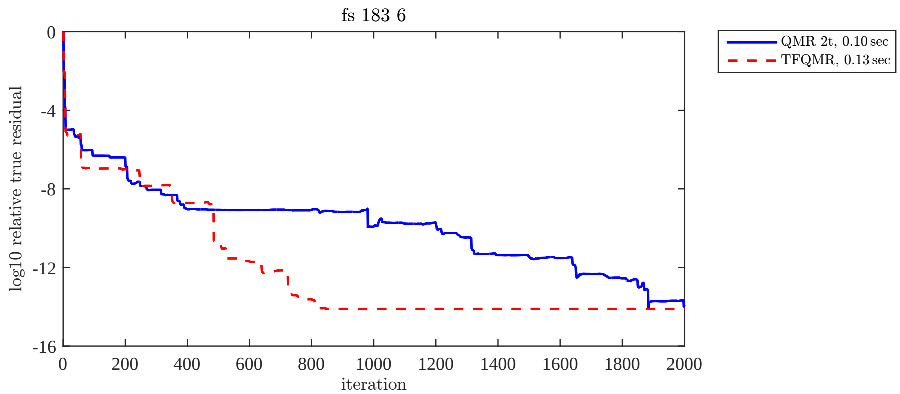

Fig. 9.19 `fs 183 6`, relative true residual norms, QMR 2t (plain), TFQMR (dashed)

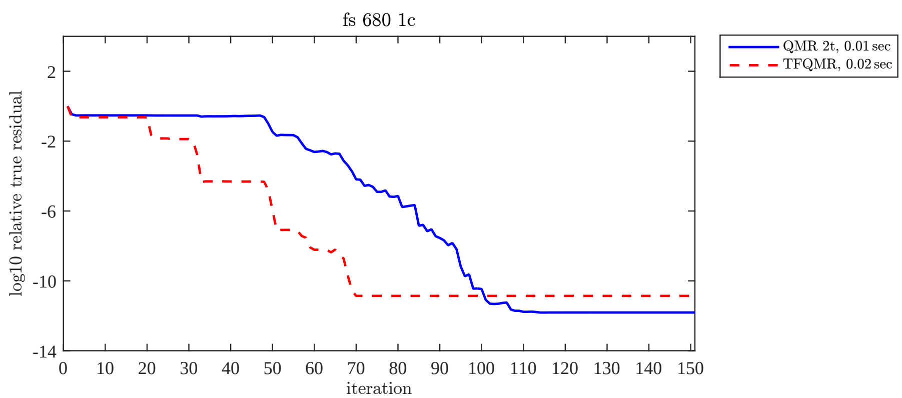

Fig. 9.20 `fs 680 1c`, relative true residual norms, QMR 2t (plain), TFQMR (dashed)

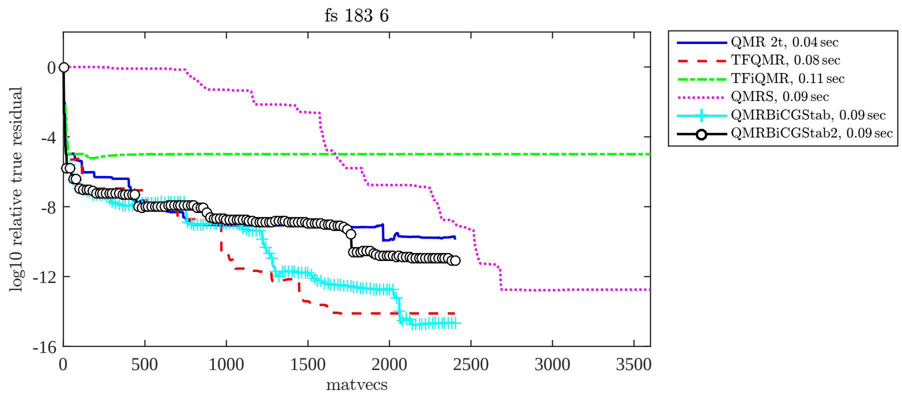

Fig. 9.21 `fs 183 6`, relative true residual norms, different QMR-like algorithms

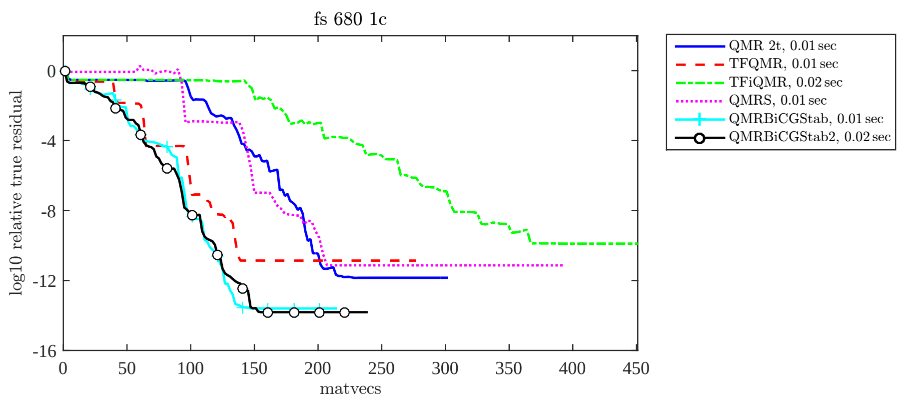

Fig. 9.22 `fs 680 1c`, relative true residual norms, different QMR-like algorithms

Chapter 10
The IDR family

10.10 Numerical examples

10.10.1 IDR

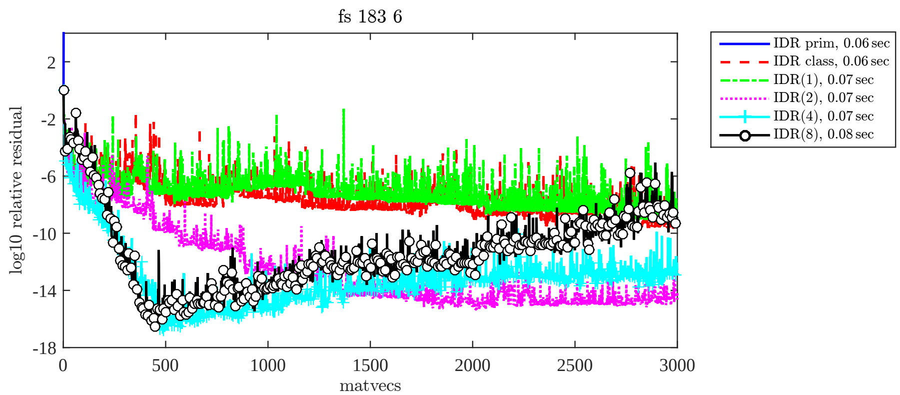

Fig. 10.1 `fs 183 6`, relative residual norms, different IDR algorithms

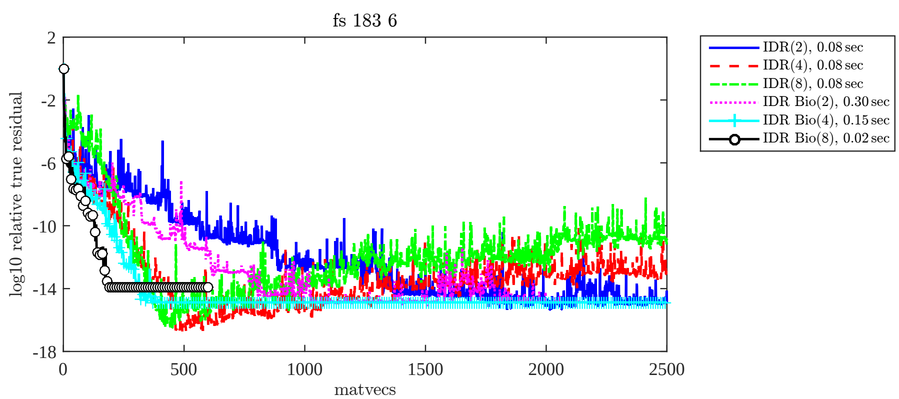

Fig. 10.2 `fs 183 6`, relative true residual norms, different IDR algorithms

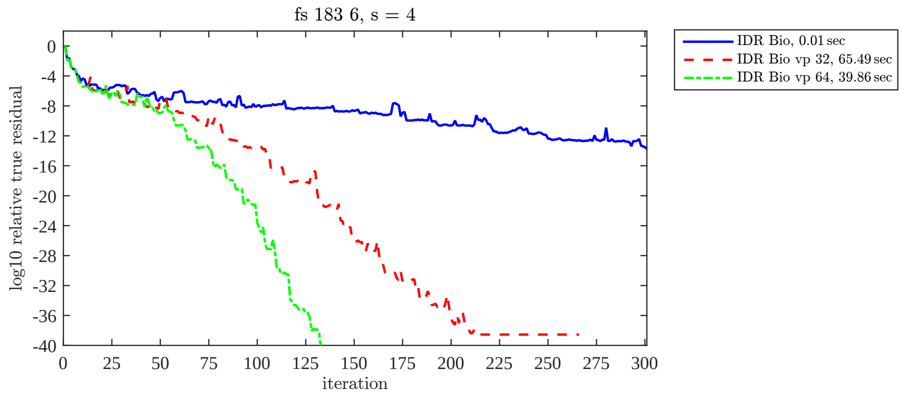

Fig. 10.3 `fs 183 6`, $\log_{10}$ of the relative true residual norm, IDR-Bio(4) (plain), IDR-Bio(4) variable precision with 32 decimal digits (dashed) and with 64 decimal digits (dot-dashed)

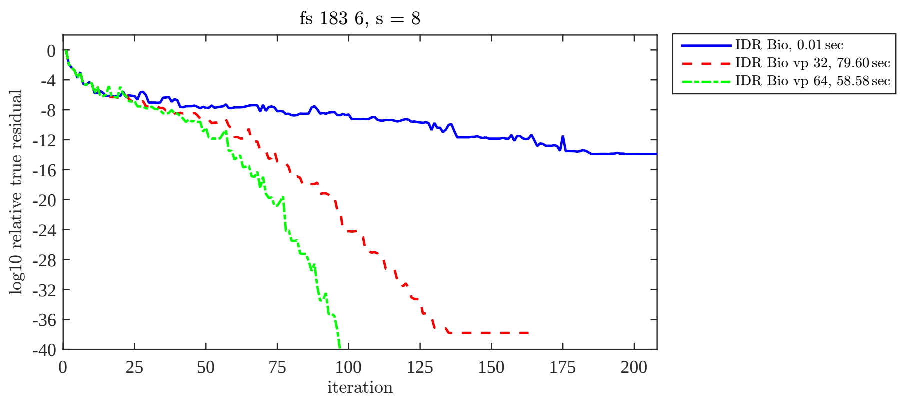

Fig. 10.4 `fs 183 6`, $\log_{10}$ of the relative true residual norm, IDR-Bio(8) (plain), IDR-Bio(8) variable precision with 32 decimal digits (dashed) and with 64 decimal digits (dot-dashed)

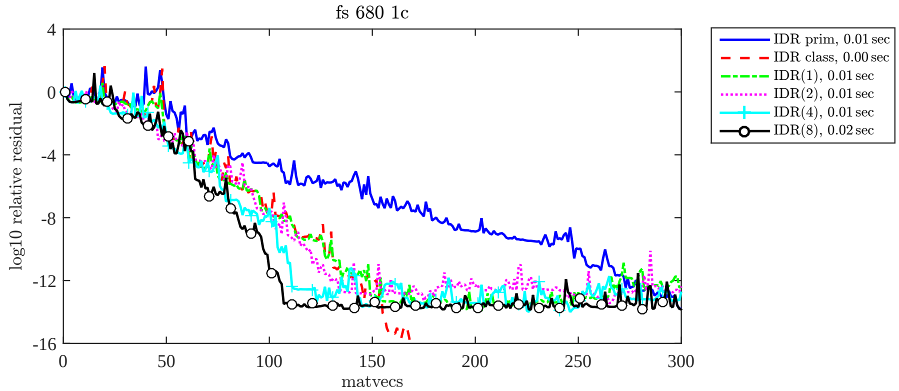

Fig. 10.5 `fs 680 1c`, relative residual norms, different IDR algorithms

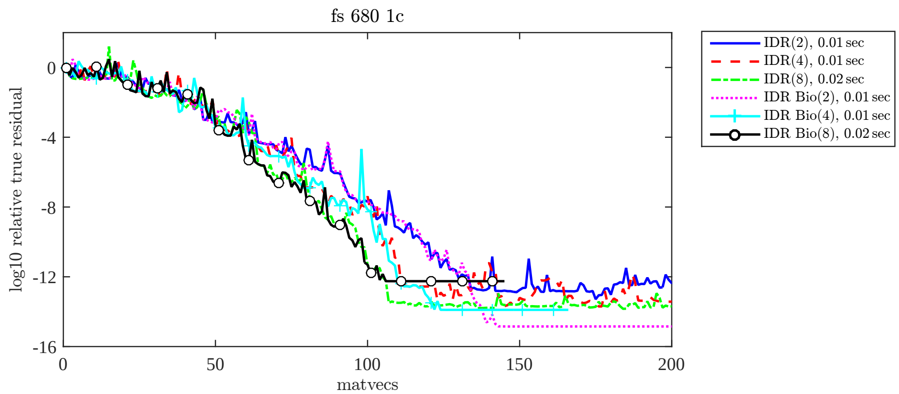

Fig. 10.6 `fs 680 1c`, relative true residual norms, different IDR algorithms

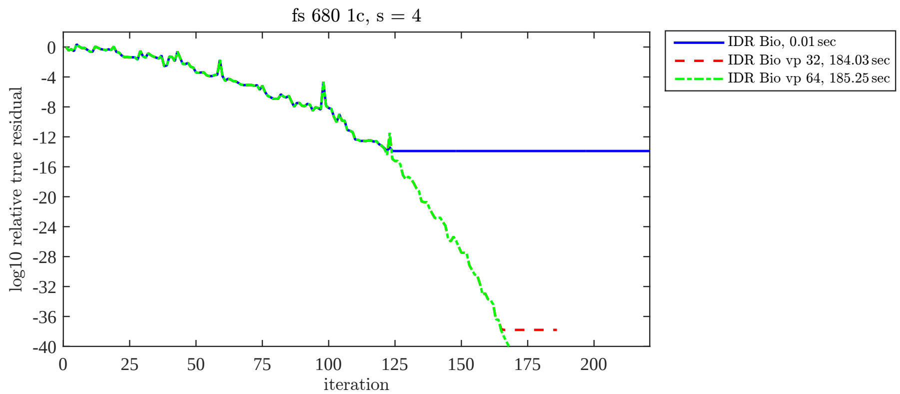

Fig. 10.7 `fs 680 1c`, $\log_{10}$ of the relative true residual norm, IDR-Bio(4) (plain), IDR-Bio(4) variable precision with 32 decimal digits (dashed) and with 64 decimal digits (dot-dashed)

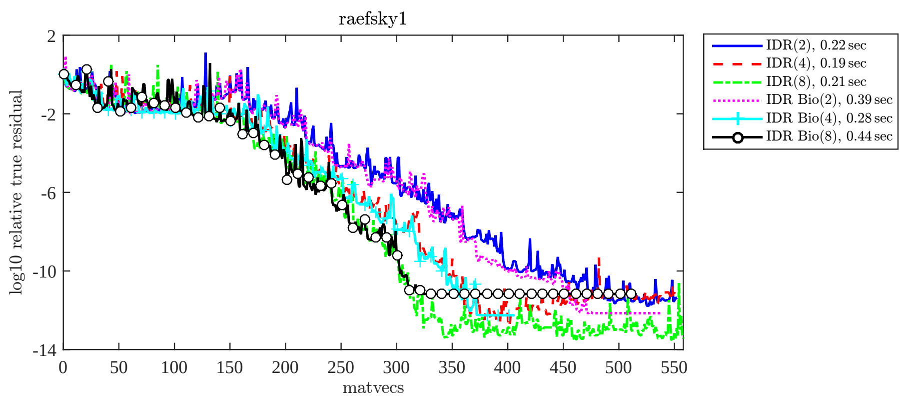

Fig. 10.8 `raefsky1`, relative true residual norms, different IDR algorithms

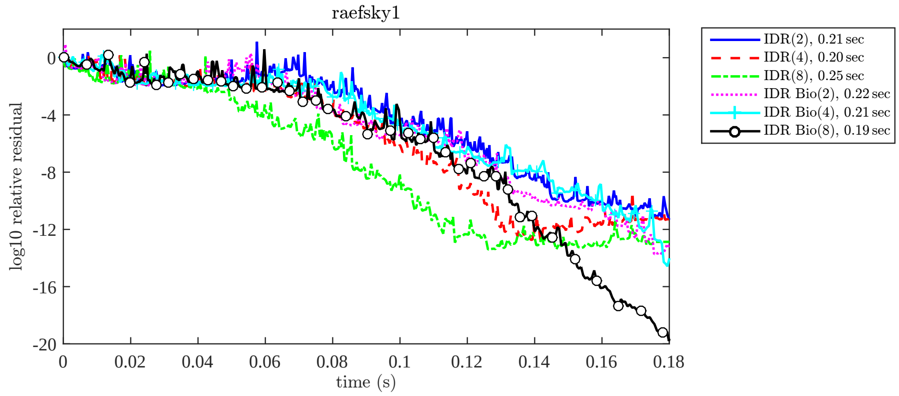

Fig. 10.9 `raefsky1`, relative residual norms, different IDR algorithms, residual norms vs time

10.10.2 Variants of IDR and IDR-QMR

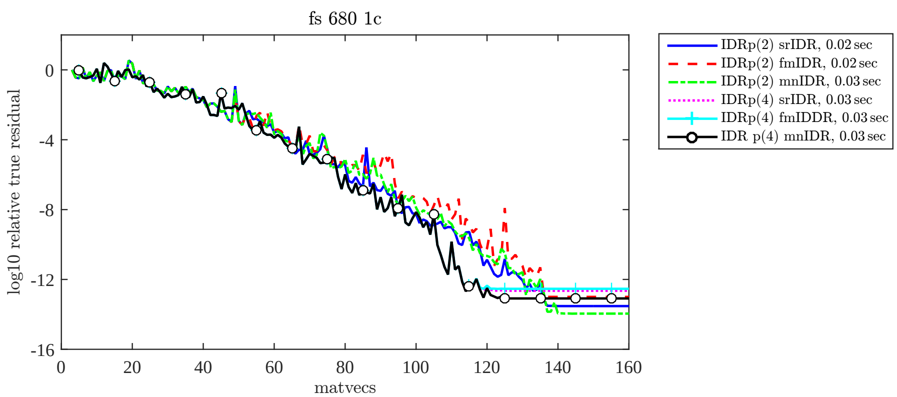

Fig. 10.10 `fs 680 1c`, relative true residual norms, different Q-OR IDR partial orthogonalization algorithms

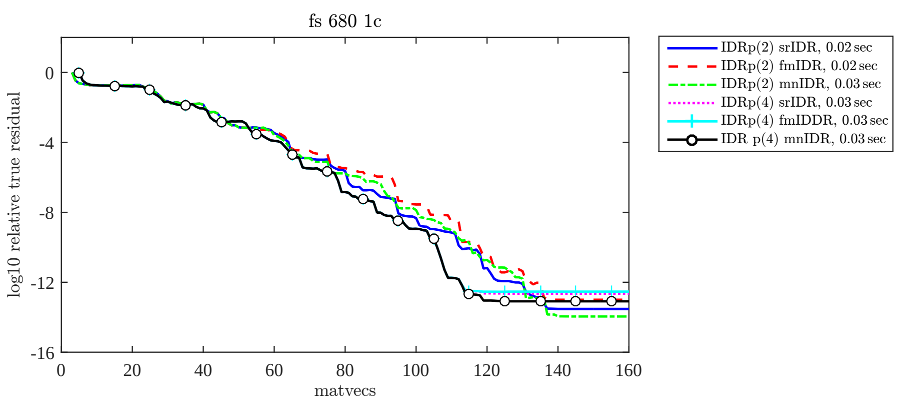

Fig. 10.11 `fs 680 1c`, relative true residual norms, different Q-MR IDR partial orthogonalization algorithms

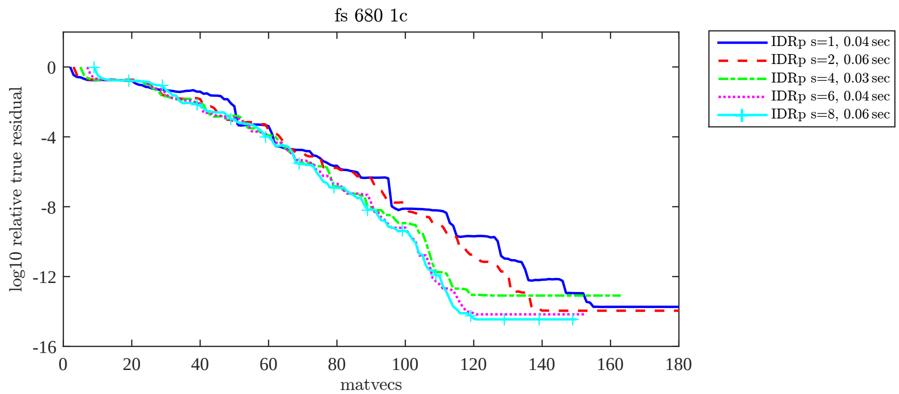

Fig. 10.12 `fs 680 1c`, relative true residual norms, Q-MR IDR partial orthogonalization mnIDR algorithms, different values of *s*

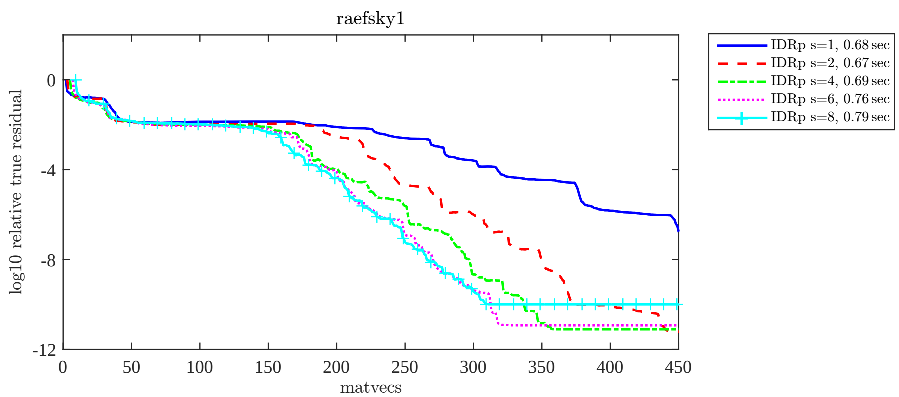

Fig. 10.13 `raefsky1`, relative true residual norms, Q-MR IDR partial orthogonalization mnIDR algorithms, different values of *s*

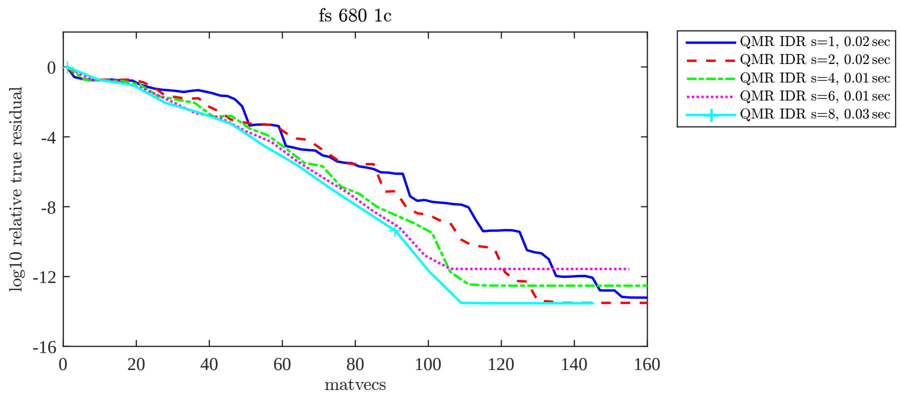

Fig. 10.14 `fs 680 1c`, relative true residual norms, Q-MR IDR algorithms from [?], different values of s

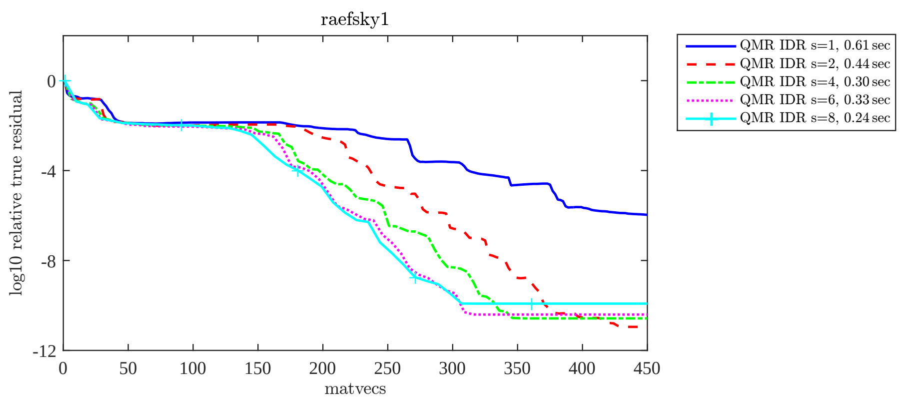

Fig. 10.15 `raefsky1`, relative true residual norms, Q-MR IDR algorithms from [?], different values of s

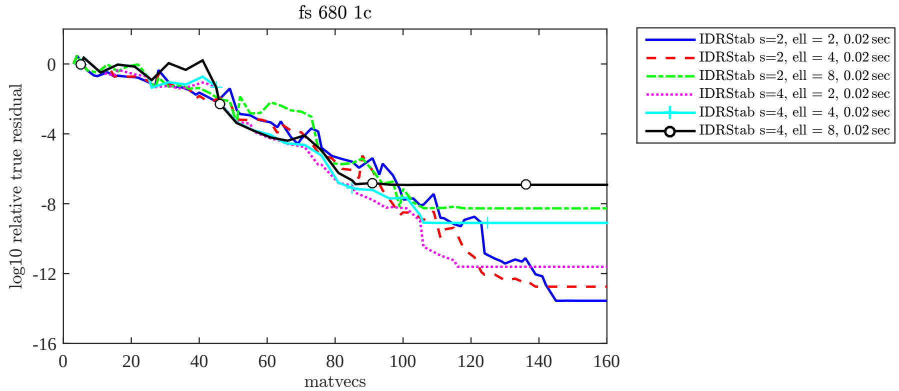

Fig. 10.16 `fs 680 1c`, relative true residual norms, IDRStab algorithms from [**?**], different values of s and ℓ

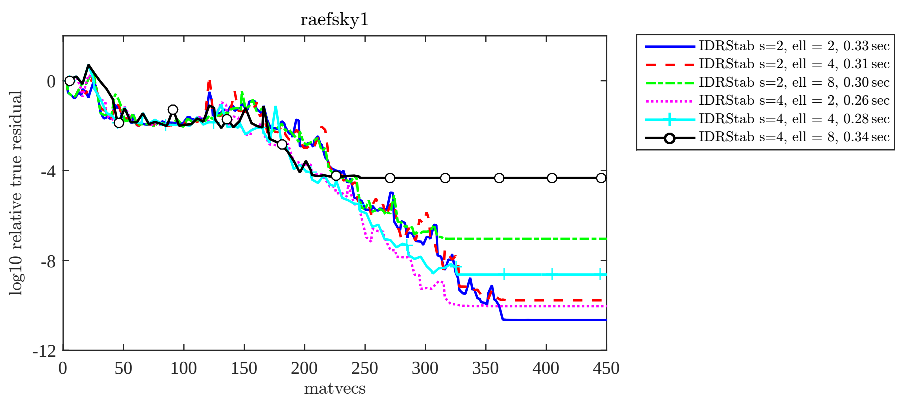

Fig. 10.17 `raefsky1`, relative true residual norms, IDRStab algorithms from [**?**], different values of s and ℓ

10.10.3 ML(k)BiCGStab

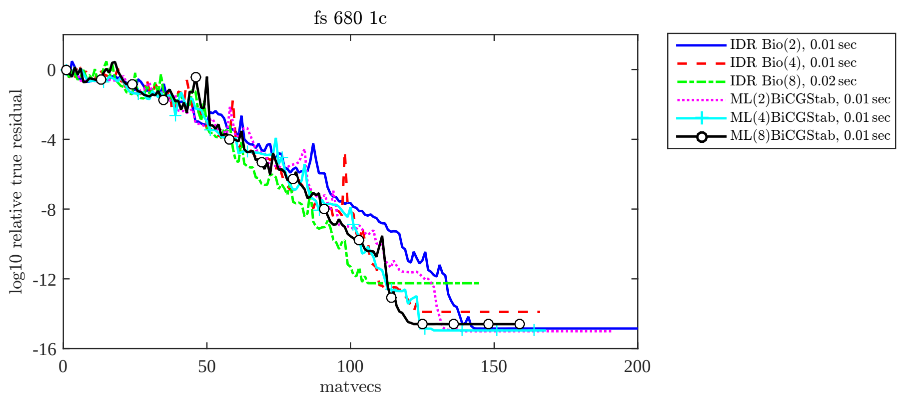

Fig. 10.18 `fs 680 1c`, relative true residual norms, IDR Bio(s) and ML(k)BiCGStab algorithms, different values of s and k

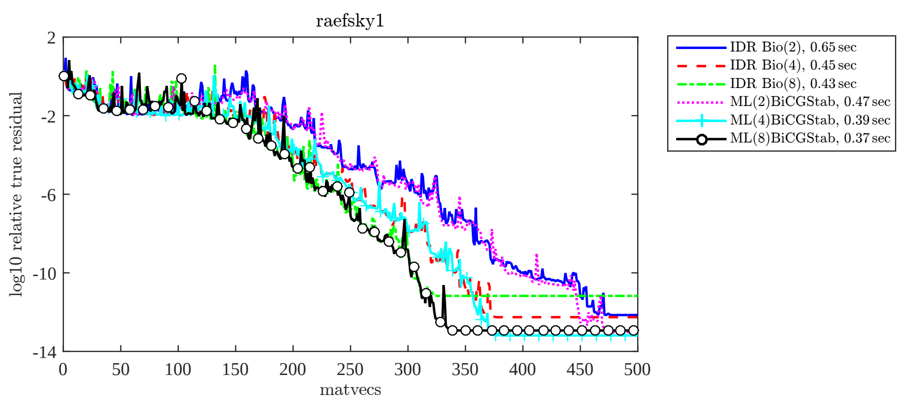

Fig. 10.19 `raefsky1`, relative true residual norms, IDR Bio(s) and ML(k)BiCGStab algorithms, different values of s and k

Chapter 11
Restart, deflation and truncation

11.1 Restarted FOM and GMRES

11.2 Prescribed convergence

11.3 Restarting techniques for FOM and GMRES

11.4 Restarted and augmented CMRH and Q-OR Opt

11.5 Truncated FOM and GMRES

11.6 Truncated Q-OR

11.7 Parallel computing

11.8 Finite precision arithmetic

11.9 Numerical experiments

11.9.1 Restarted GMRES without preconditioning

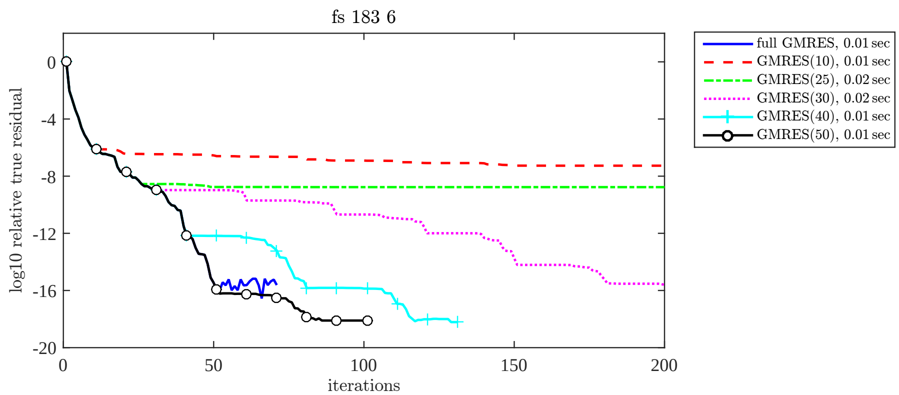

Fig. 11.1 fs 183 6, relative true residual norms, GMRES-MGS(m), different values of m

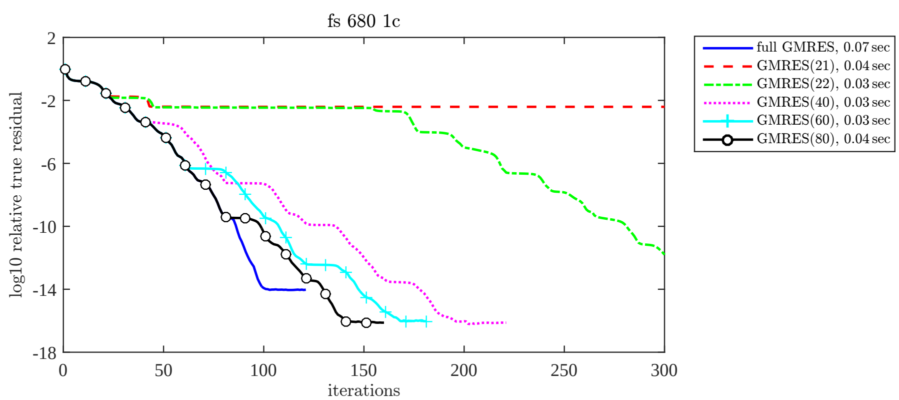

Fig. 11.2 fs 680 1c, relative true residual norms, GMRES-MGS(m), different values of m

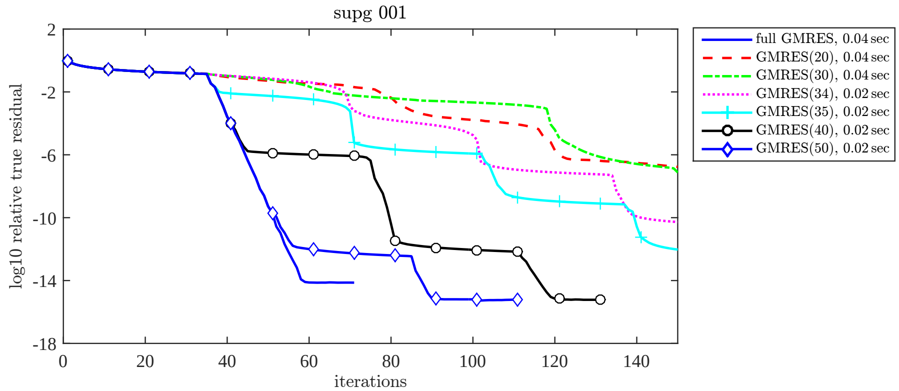

Fig. 11.3 supg 001, relative true residual norms, GMRES-MGS(m), different values of m

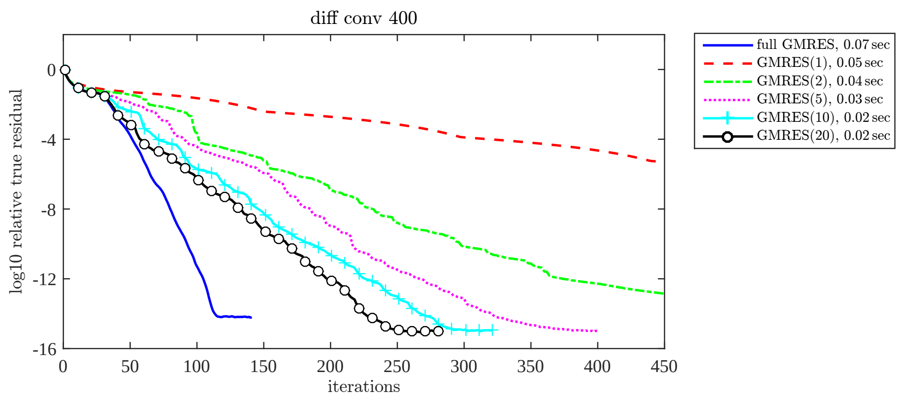

Fig. 11.4 diff conv 400, relative true residual norms, GMRES-MGS(m), different values of m

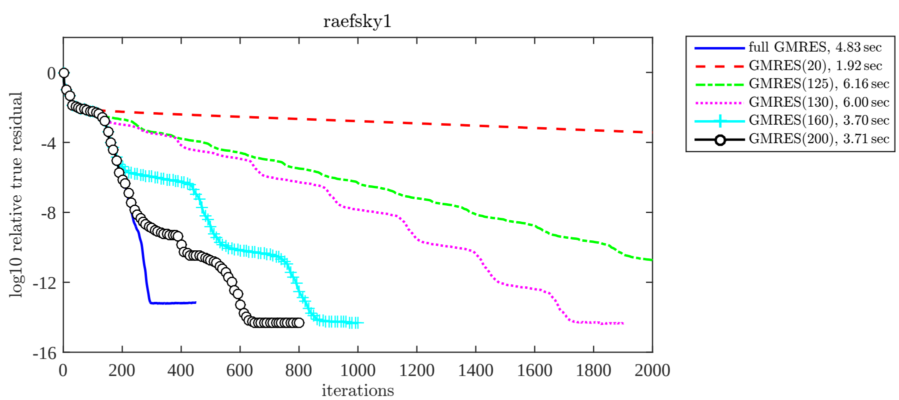

Fig. 11.5 raefsky1, relative true residual norms, GMRES-MGS(m), different values of m

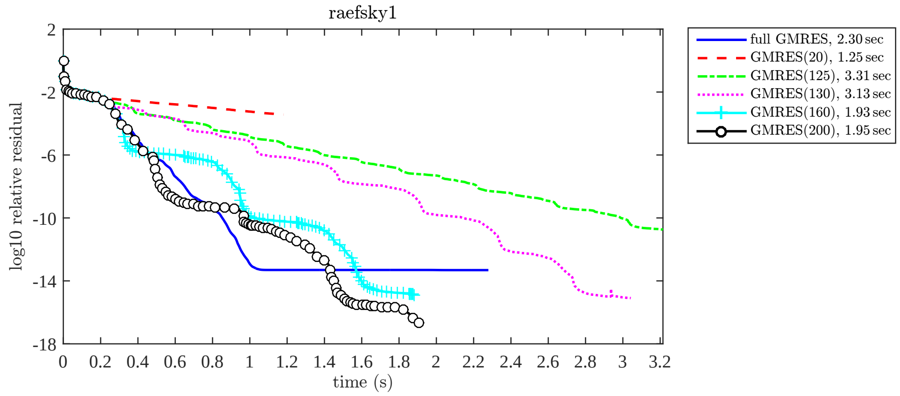

Fig. 11.6 raefsky1, relative residual norms vs time, GMRES-MGS(m), different values of m

11.9.2 Restarted GMRES with preconditioning

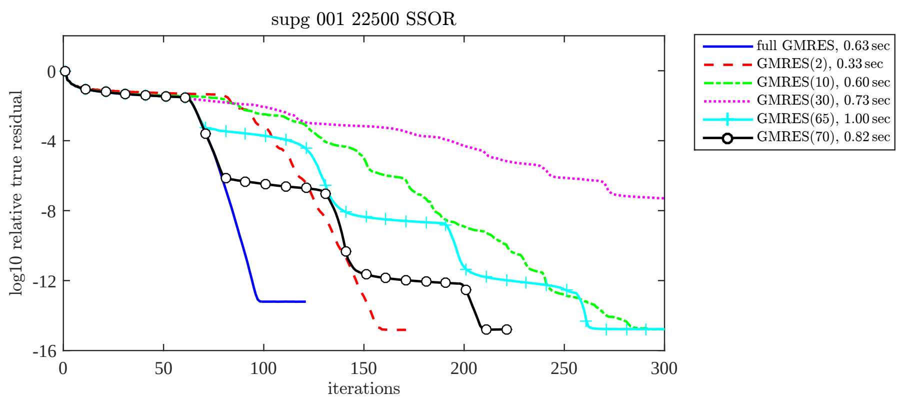

Fig. 11.7 supg 001 22500, relative true residual norms, GMRES-MGS(m) with SSOR preconditioning, different values of m

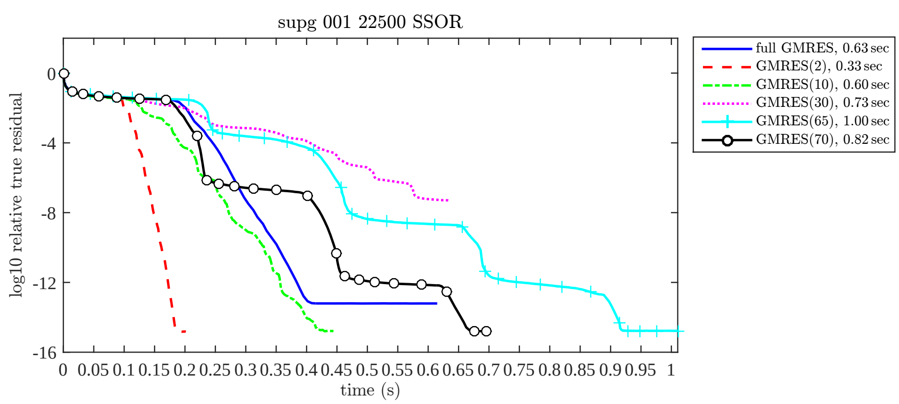

Fig. 11.8 supg 001 22500, relative true residual norms vs time, GMRES-MGS(m) with SSOR preconditioning, different values of m

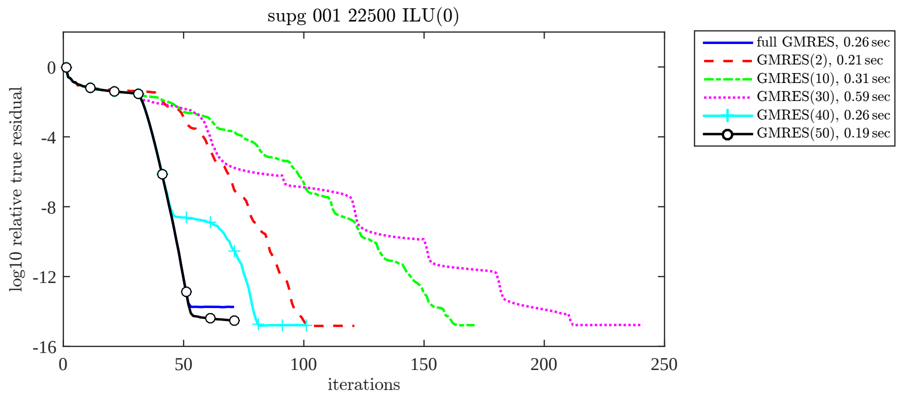

Fig. 11.9 supg 001 22500, relative true residual norms, GMRES-MGS(m) with ILU(0) preconditioning, different values of m

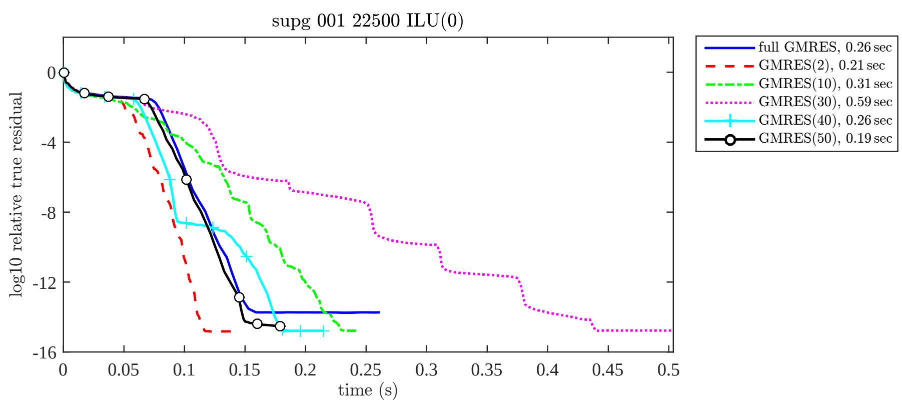

Fig. 11.10 supg 001 22500, relative true residual norms vs time, GMRES-MGS(m) with ILU(0) preconditioning, different values of m

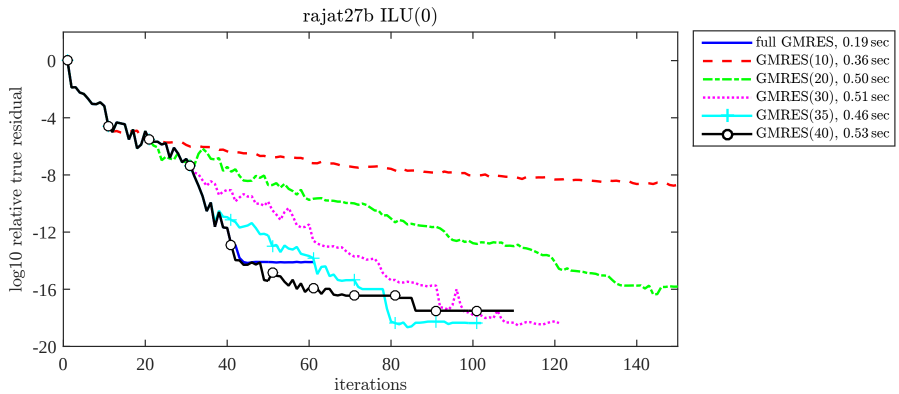

Fig. 11.11 rajat27b, relative true residual norms, GMRES-MGS(m) with ILU(0) preconditioning, different values of m

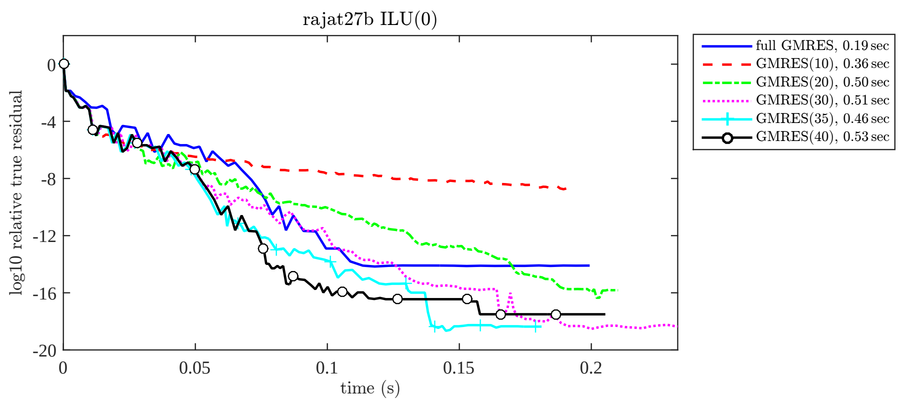

Fig. 11.12 rajat27b, relative true residual norms vs time, GMRES-MGS(m) with ILU(0) preconditioning, different values of m

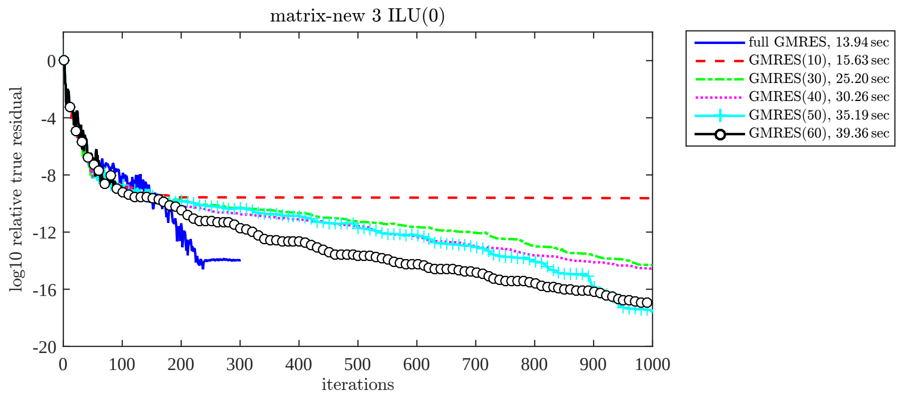

Fig. 11.13 matrix-new 3, relative true residual norms, GMRES-MGS(m) with ILU(0) preconditioning, different values of m

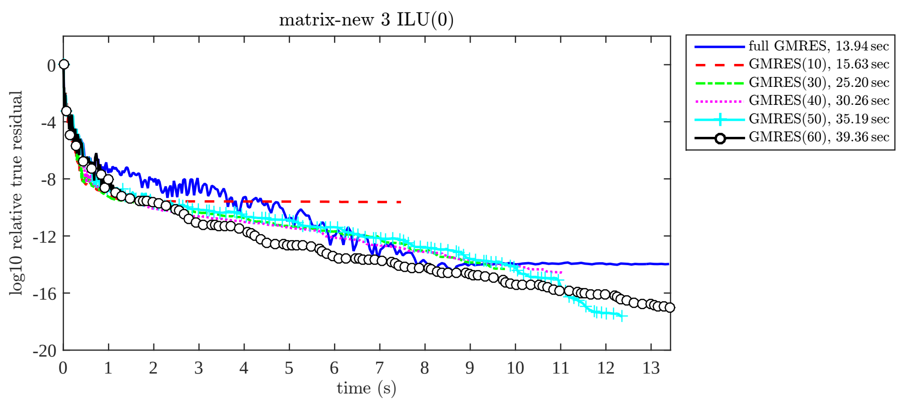

Fig. 11.14 matrix-new 3, relative true residual norms vs time, GMRES-MGS(m) with ILU(0) preconditioning, different values of m

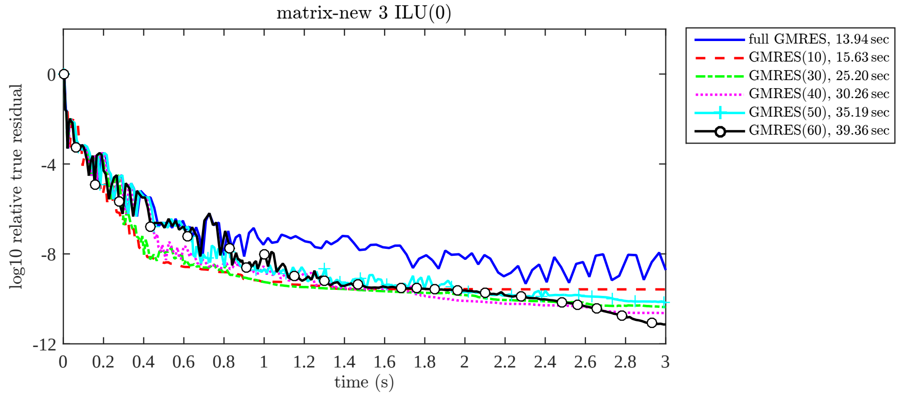

Fig. 11.15 matrix-new 3, relative true residual norms vs time, GMRES-MGS(m) with ILU(0) preconditioning, different values of m

11.9.3 Restarting with deflation and augmentation without preconditioning

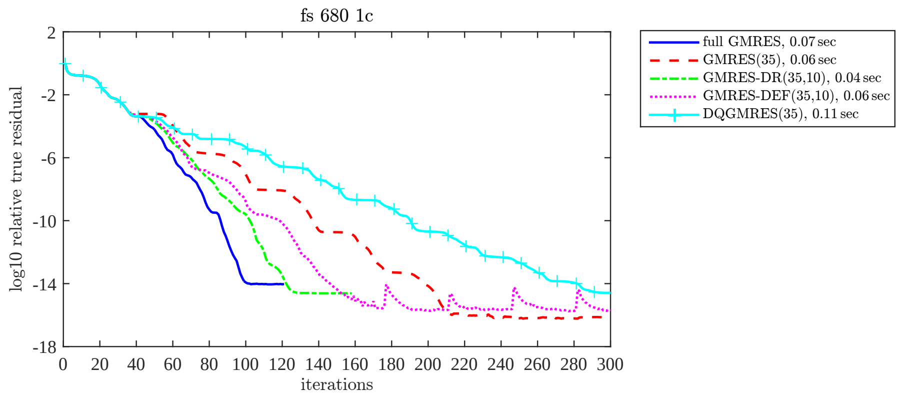

Fig. 11.16 fs 680 1c, relative true residual norms, full GMRES and GMRES(m) with different restarting techniques

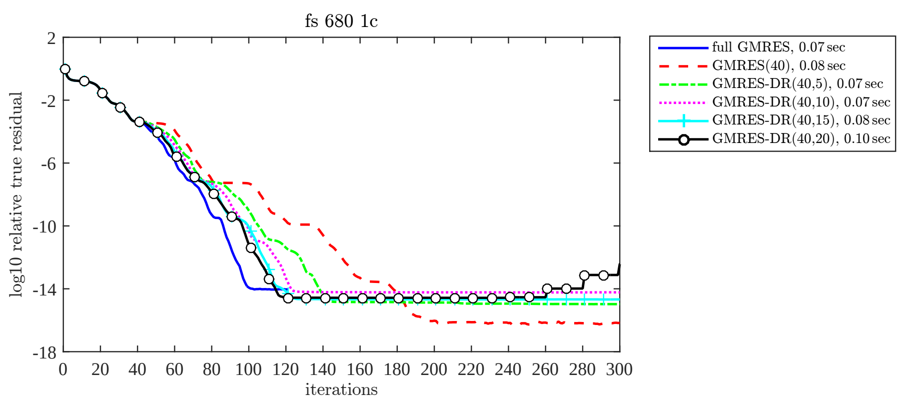

Fig. 11.17 fs 680 1c, relative true residual norms, full GMRES, GMRES(40) and GMRES-DR(40) with different number of harmonic Ritz vectors

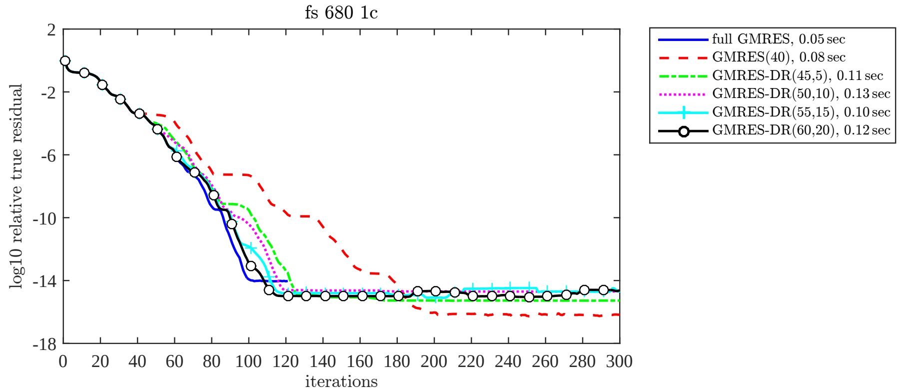

Fig. 11.18 fs 680 1c, relative true residual norms, full GMRES, GMRES(40) and GMRES-DR(m) with different number of harmonic Ritz vectors

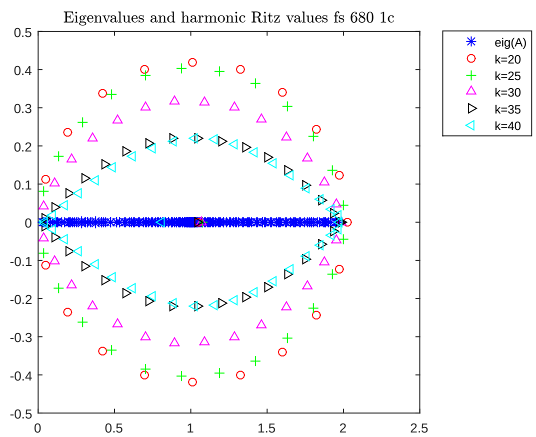

Fig. 11.19 fs 680 1c, eigenvalues and harmonic Ritz values, iterations 20:5:40

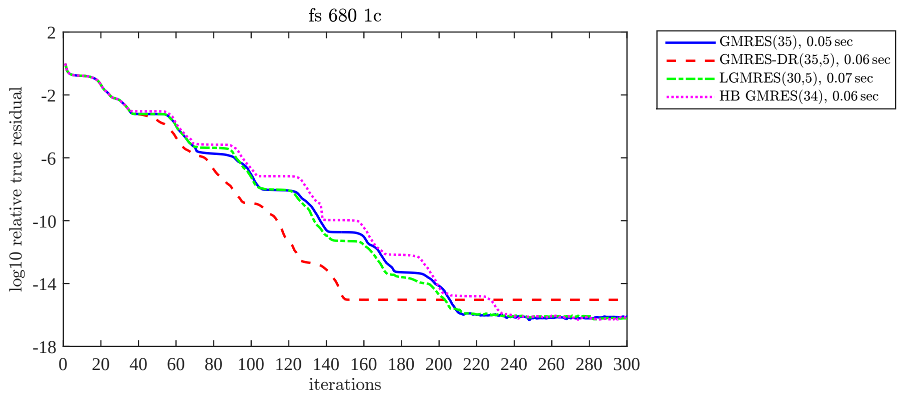

Fig. 11.20 fs 680 1c, relative true residual norms, GMRES(35), GMRES-DR(35,5), LGM-RES(30,5) and HBGMRES(34)

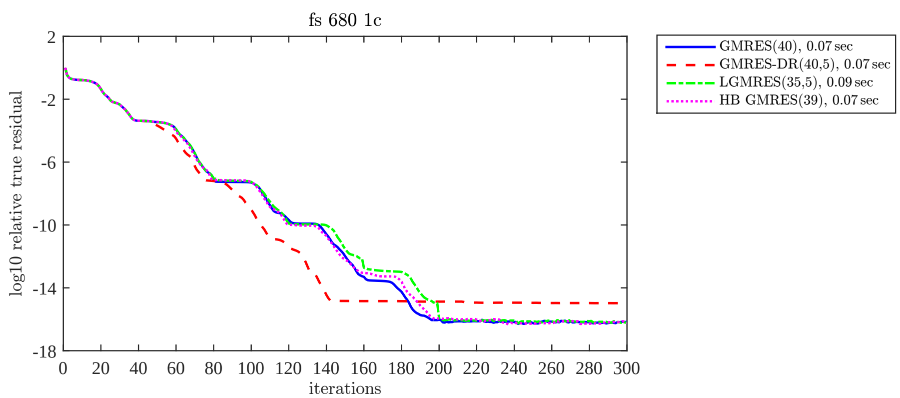

Fig. 11.21 fs 680 1c, relative true residual norms, GMRES(40), GMRES-DR(40,5), LGM-RES(35,5) and HBGMRES(39)

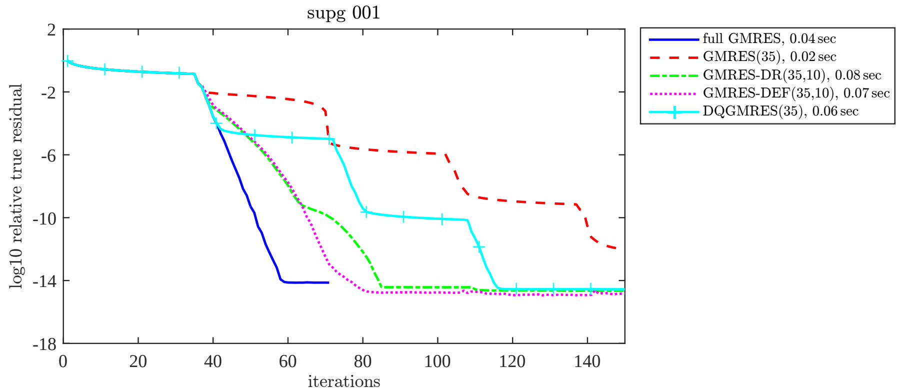

Fig. 11.22 supg 001, $n = 1225$, relative true residual norms, full GMRES and GMRES(m) with different restarting techniques

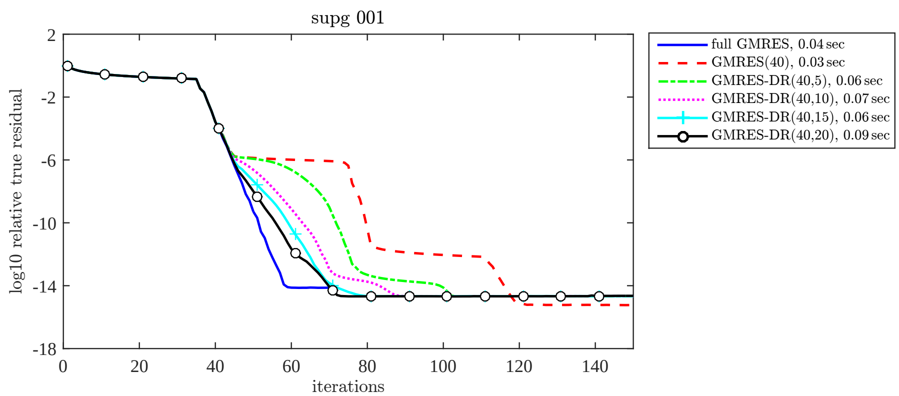

Fig. 11.23 supg001, $n = 1225$, relative true residual norms, full GMRES, GMRES(40) and GMRES-DR(40) with different number of harmonic Ritz vectors

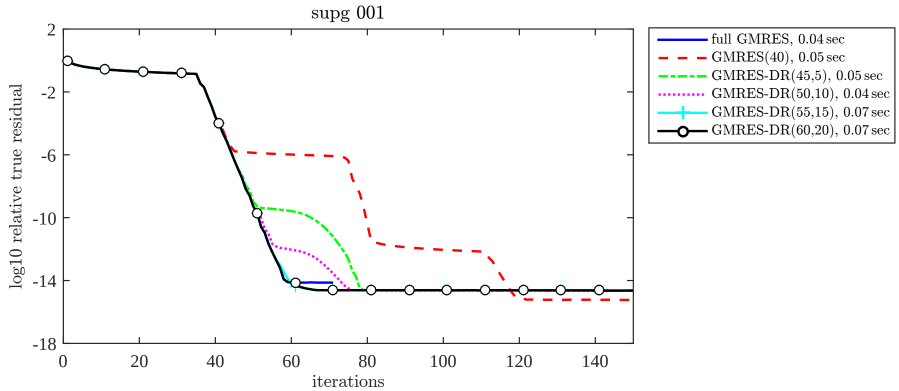

Fig. 11.24 supg001, $n = 1225$, relative true residual norms, full GMRES, GMRES(40) and GMRES-DR(m) with different number of harmonic Ritz vectors

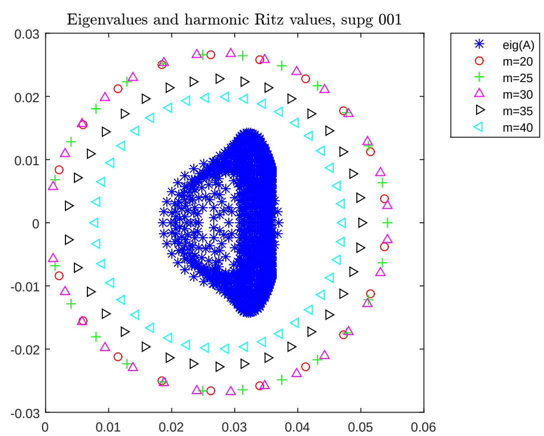

Fig. 11.25 supg 001, $n = 1225$, eigenvalues and harmonic Ritz values, iterations 20:5:40

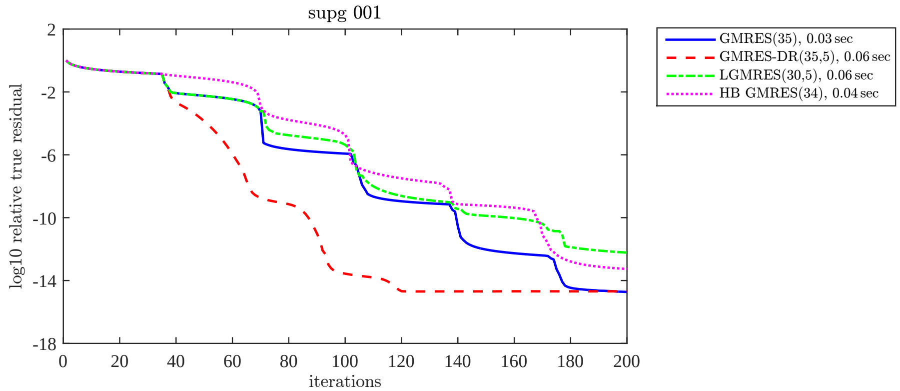

Fig. 11.26 supg 001, $n = 1225$, relative true residual norms, GMRES(35), GMRES-DR(35,5), LGMRES(30,5) and HBGMRES(34)

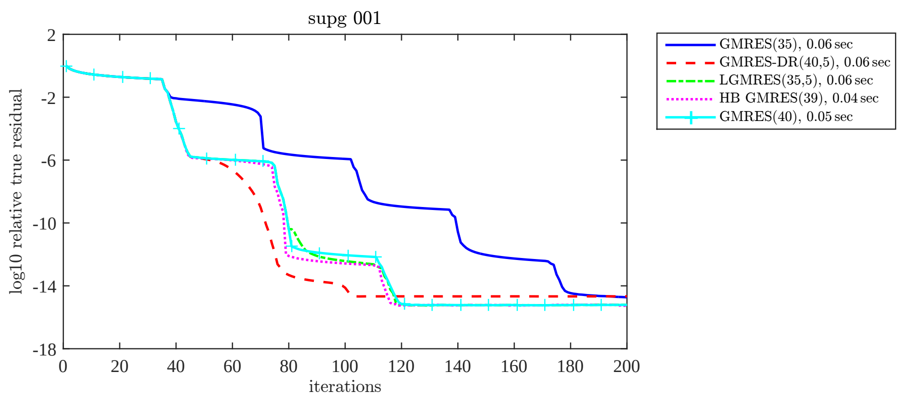

Fig. 11.27 supg 001, $n = 1225$, relative true residual norms, GMRES(35), GMRES-DR(40,5), LGMRES(35,5), HBGMRES(39) and GMRES(40)

11.9.4 Restarting with deflation and augmentation with preconditioning

11.9.5 Truncated Q-OR

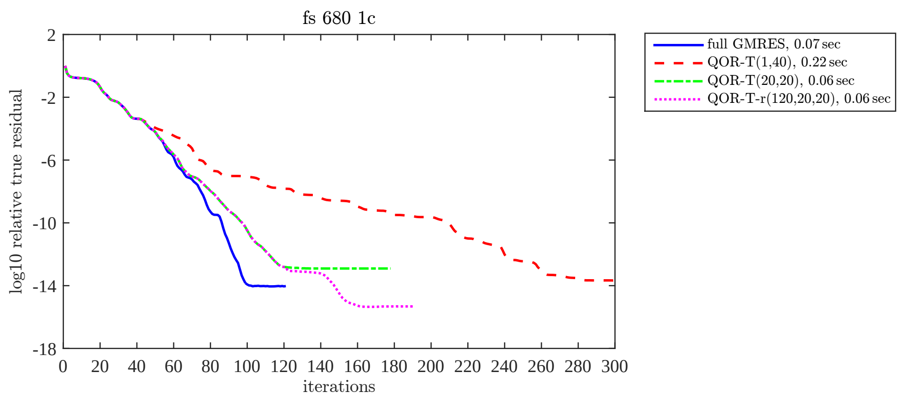

Fig. 11.28 fs 680 1c, relative true residual norms, full GMRES, QOR-T(1,40), QOR-T(20,20) and QOR-T(20,20) with restart at $k = 120$

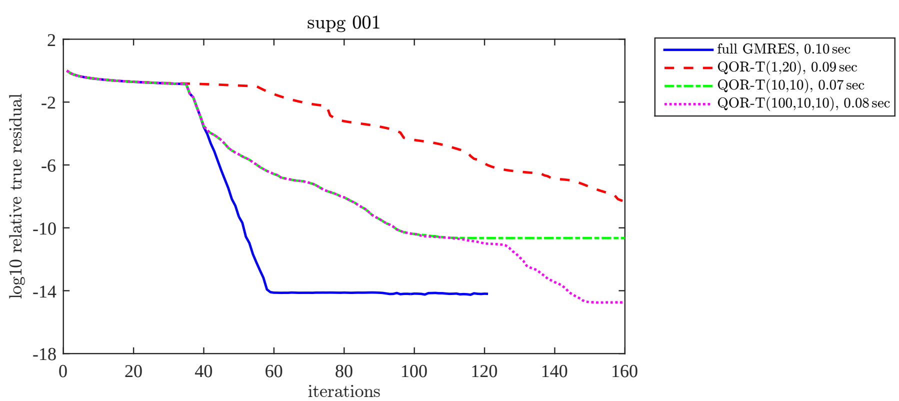

Fig. 11.29 supg 001, $n = 1225$, relative true residual norms, full GMRES, QOR-T(1,20), QOR-T(10,10) and QOR-T(10,10) with restart at $k = 100$

Chapter 12

Related topics

12.1 FGMRES

12.2 GCRO

12.3 Relaxation for matrix-vector products

12.4 Systems with multiple right-hand sides

12.5 Shifted linear systems

12.6 Singular systems

12.7 Least squares problems

12.8 Ill-posed problems

12.9 Eigenvalue computations and rational Krylov methods

12.10 Functions of matrices

12.11 Minimum error methods

12.12 Residual replacement techniques

12.13 Residual smoothing techniques

12.14 Hybrid methods

12.15 CGNE and CGNR

12.16 USYMLQ and USYMQR

Chapter 13
Numerical comparisons of methods

13.1 Introduction

13.2 Small matrices

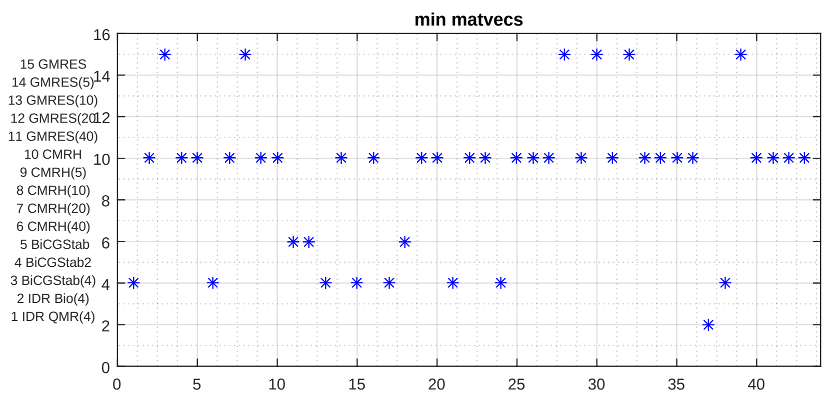

Fig. 13.1 Small matrices, minimum number of matvecs, $\epsilon = 10^{-6}$

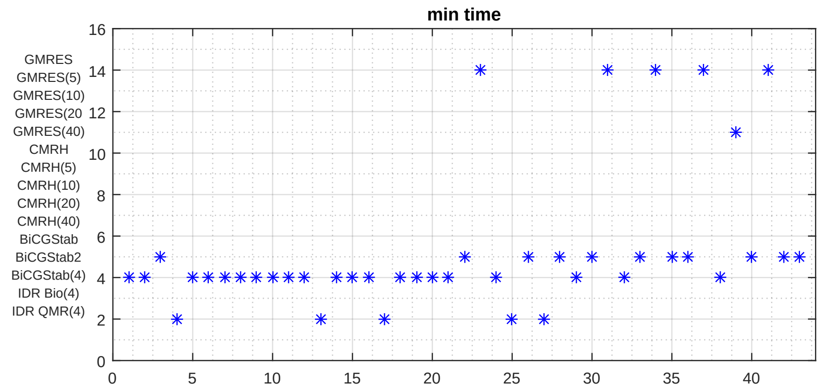

Fig. 13.2 Small matrices, minimum computing time, $\epsilon = 10^{-6}$

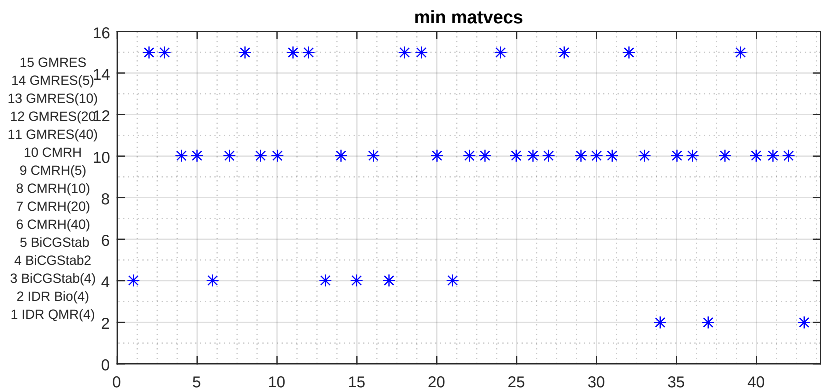

Fig. 13.3 Small matrices, minimum number of matvecs, $\epsilon = 10^{-10}$

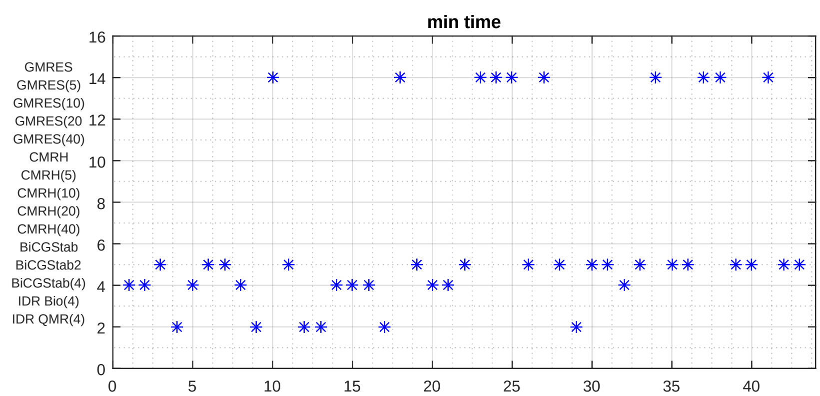

Fig. 13.4 Small matrices, minimum computing time, $\epsilon = 10^{-10}$

13.3 Larger matrices

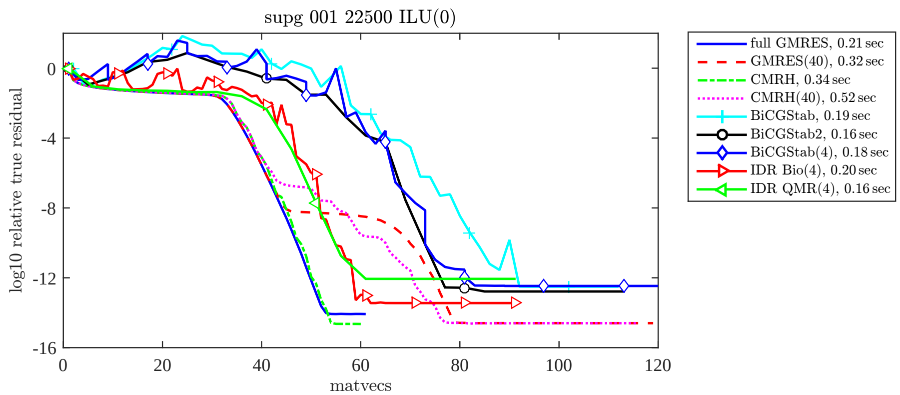

Fig. 13.5 supg 001 22500, relative true residual norms vs matvecs, ILU(0) preconditioning

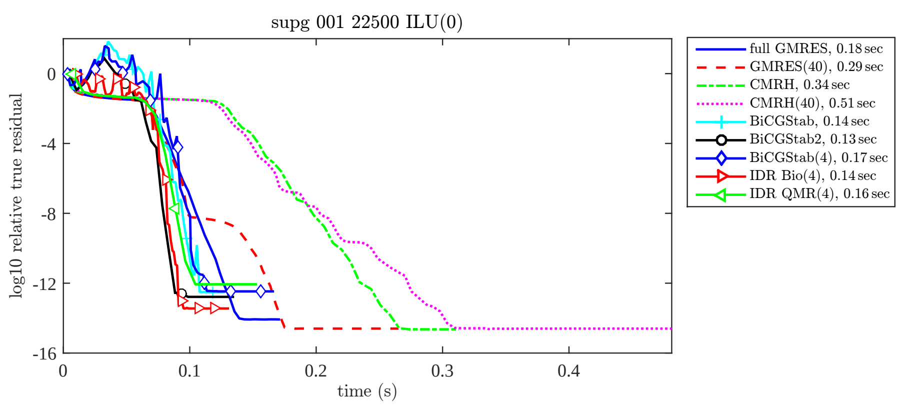

Fig. 13.6 supg 001 22500, relative true residual norms vs time, ILU(0) preconditioning

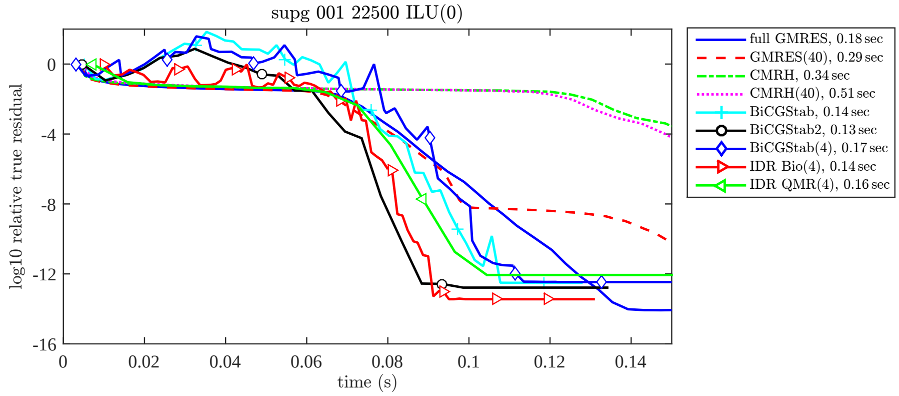

Fig. 13.7 supg 001 22500, relative true residual norms vs time, zoom, ILU(0) preconditioning

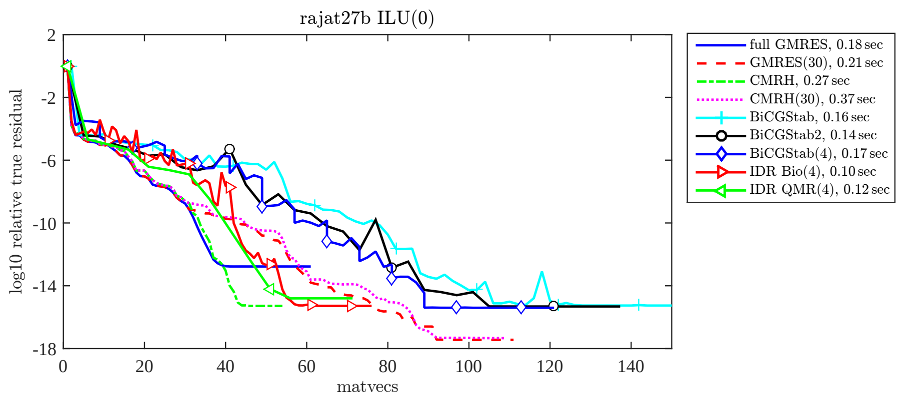

Fig. 13.8 rajat27b, relative true residual norms vs matvecs, ILU(0) preconditioning

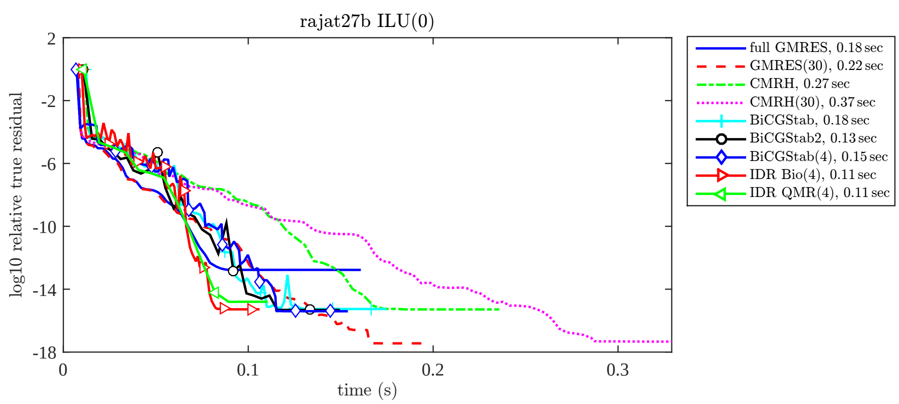

Fig. 13.9 rajat27b, relative true residual norms vs time, ILU(0) preconditioning

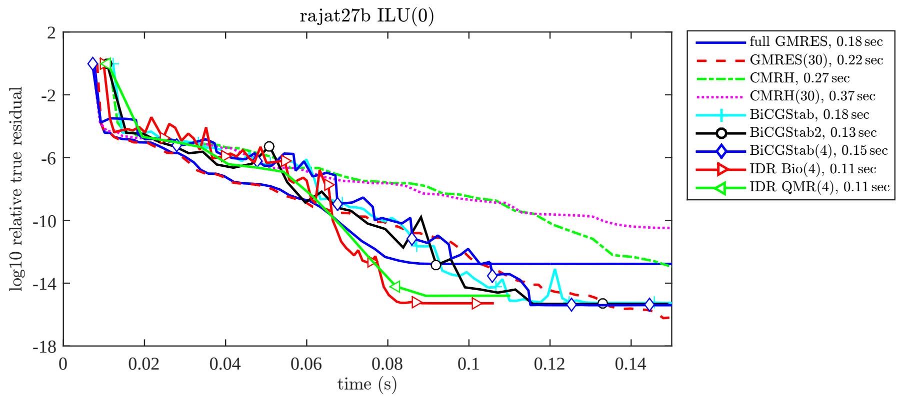

Fig. 13.10 rajat27b, relative true residual norms vs time, zoom, ILU(0) preconditioning

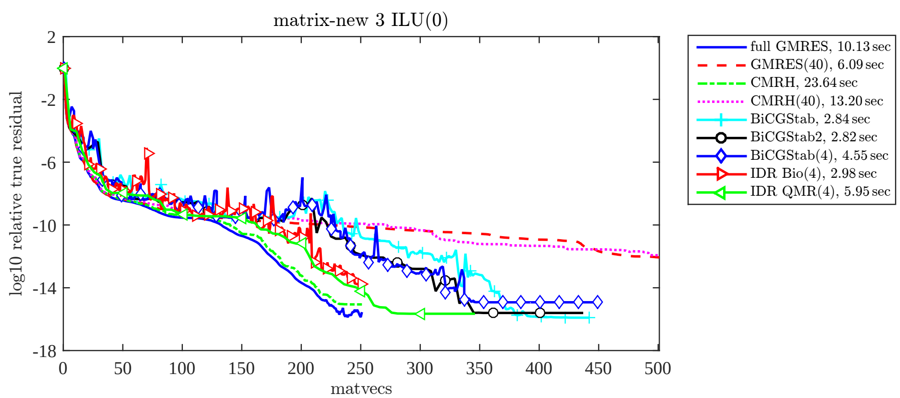

Fig. 13.11 matrix-new 3, relative true residual norms vs matvecs, ILU(0) preconditioning

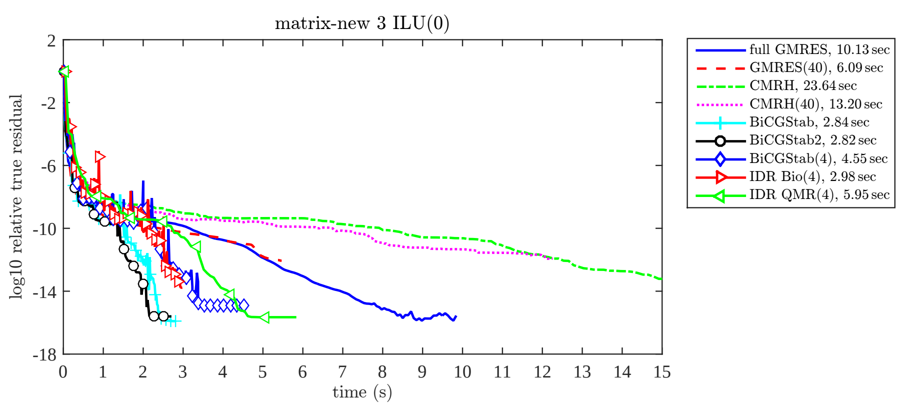

Fig. 13.12 matrix-new 3, relative true residual norms vs time, ILU(0) preconditioning

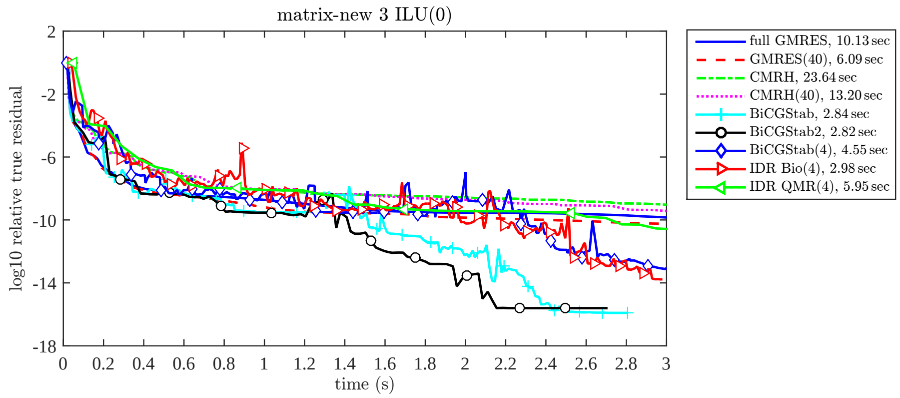

Fig. 13.13 matrix-new 3, relative true residual norms vs time, zoom, ILU(0) preconditioning

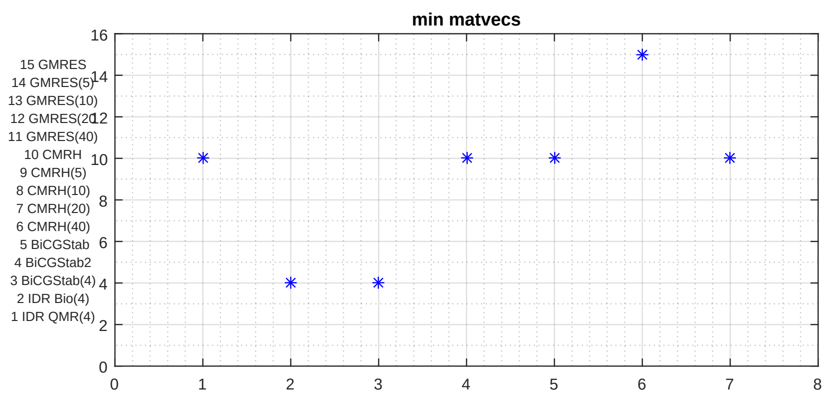

Fig. 13.14 Large matrices, minimum number of matvecs, $\epsilon = 10^{-6}$

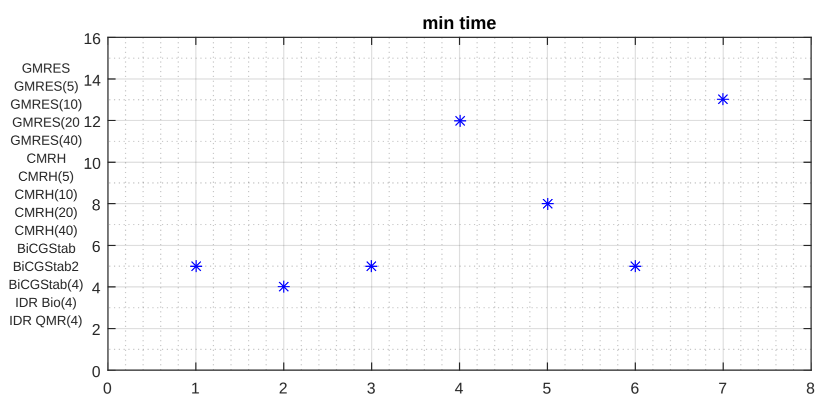

Fig. 13.15 Large matrices, minimum computing time, $\epsilon = 10^{-6}$

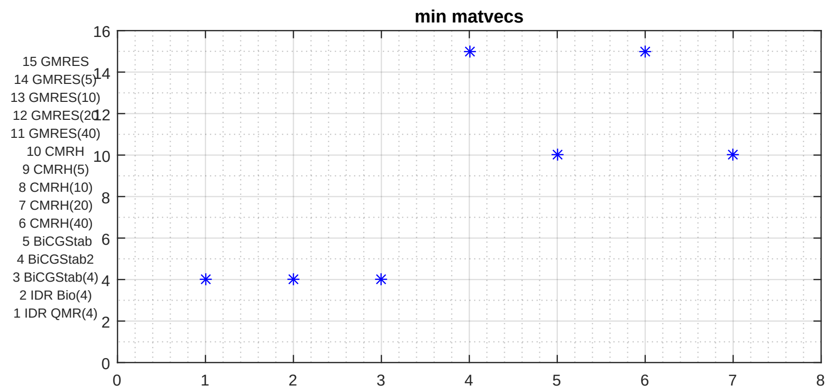

Fig. 13.16 Large matrices, minimum number of matvecs, $\epsilon = 10^{-10}$

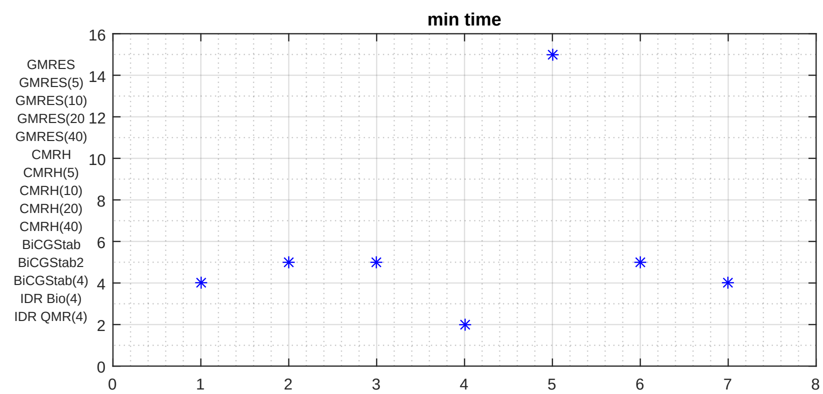

Fig. 13.17 Large matrices, minimum computing time, $\epsilon = 10^{-10}$